CHIBA UNIVERSITY

INVESTIGATION OF CHANGES IN COOKED RICE ATTRIBUTES BY ADDING VARIOUS MANIPULATIONS AND SUPPLEMENTS

LIN WANG

GRADUATE SCHOOL OF HORTICULTURE

CHIBA UNIVERSITY

March 2025

CONTENTS

目次

ABSTRACT

This study investigated the physicochemical modifications of cooked rice caused by adding various supplements (rapeseed oil, dried chili pepper, and wasabi powder). The physicochemical and digestive properties were examined by applying multiple analysis techniques and how they affected cooked rice quality, including starch digestibility. All samples adding supplements showed an increase in surface firmness (0.77-0.95 N) and a decrease in thickness (2.23-2.35 mm) and surface adhesiveness (1.43-7.22 N). Cooked rice adding rapeseed oil showed the opposite trend for the overall firmness against others and retard the starch hydrolysis rate. That could be considered due to its reinforced structure and the presence of a lipid layer, which inhibits the penetration of enzymes as physical barriers. A decrease in hydrolysis rate was also observed in the samples adding dried chili pepper and wasabi powders. This might be attributed to the effects of inhibiting enzymes by releasing substances. The content of resistant starch (RS) and slowly digested starch (SDS) was increased in all samples by adding supplements. Lipid has crucial applications for improving the quality of starchy products during heat-processing. Herein, the influence of lipid modification and thermal treatment on the physicochemical properties and starch digestibility of cooked rice prepared with varied addition manipulations was further investigated. Rice bran oil (RO) and MCT oil (MO) manipulations were performed either before (RB, MB) or after (RA, MA) cooking. Gas Chromatography-Mass Spectrometry (GC-MS) was applied to determine the fatty acid (FA) profiles. Nutritional quality was analyzed by quantifying total phenolics, atherogenic (AI), and thrombogenic (TI) indices. All complexes exhibited higher surface firmness, a soft core, and less adhesive. The lowest glycemic response was observed in the RB sample, whereas the highest complexing index (CI) was observed in the RA sample, indicating that the dense molecular configuration of complexes that could resist enzymatic digestion was more critical than the quantity of complex formation. Despite the damage caused by mass and heat transfer, physical barrier, intact granule forms, and strengthened dense structure were the central contributors affecting the digestion characteristics of lipid-starch complexes.

ABSTRACT (日本語)

本研究では、各種サプリメント（数種類の油脂、唐辛子粉、ワサビ粉）の添加が米飯の理化学的特性および糖質消化性に及ぼす影響を調査、検討した。唐辛子粉およびワサビ粉を添加した米飯は、粒表面かたさが増加（0.77 ～ 0.95 N）した反面、厚さ（2.23 ～ 2.35 mm）および表面付着性（1.43 ～ 7.22 N）の減少が確認された。菜種油を添加した米飯は、粒のかたさが低下するとともに加水分解速度も低下した。加水分解速度の低下は唐辛子粉およびわさび粉を添加した米飯でも観察された。以上の結果は、粒構造のかたさ変化に加えて菜種油による油膜もしくは添加した物質が消化酵素の浸透阻害を誘発したことが原因であると考えられた。同様に含有デンプンの特性を分析した結果、すべてのサプリメント添加サンプルで難消化性デンプン（RS）および緩消化性デンプン（SDS）の含有量が増加した。以上の結果から、添加成分がデンプンの分子構造や米飯の粒構造に影響を及ぼすことで米飯の品質に関わる特性を変化させることが示された。それらの結果に基づき、油脂の添加が米飯の物理化学的性質と糖質消化性に及ぼす影響を詳細に調査、検討した。油脂として、米ぬか油（RO）および MCT 油（MO）を用い、調理前（RB、MB）または調理後（RA、MA）のいずれかの時点で添加した。脂肪酸（FA）プロファイルの決定にはガスクロマトグラフィー質量分析法（GC-MS）を適用した。また処理された米飯の総フェノール類、アテローム生成（AI）、および血栓生成（TI）指数も分析、定量化した。実験の結果、いずれの油脂添加でも粒表面かたさが増加する半面、粒のかたさおよび付着性の低下を示した。一方、RB サンプルは糖質消化性の低下が、RA サンプルでは複合体形成指数（CI）の増加が確認された。これらの結果は、油脂ーデンプン複合体の分子的な構造特性が複合体の形成量よりも消化酵素の作用に関与する可能性があることを示していると考えられた。本研究により、炊飯時の機械力学的および熱力学的な作用によって粒構造の損傷が生じたとしても、油脂などの添加サプリメントによる物理的な消化酵素に対するバリア性や脂質ーデンプン複合体の方が米飯の糖質消化特性により大きな影響を及ぼすことが明らかとなった。

LIST OF TABLES

LIST OF FIGURES

CHAPTER 1

INTRODUCTION

1.1 Background

Rice, along with wheat and corn, is one of the major cereals all over the world. It primarily consists of starch which has been widely regarded as energy source for human nutrition (Lehmann and Robin, 2007). However, due to its high proportion of rapidly digested starch (RDS), white rice is classified as a high glycemic index (GI) food with a GI index of 83.40 ± 15.93, which may increase the risk of metabolic syndromes, such as obesity and cardiovascular disease (Kaur et al., 2016; Atkinson et al., 2021). To date, many strategies are being explored regarding the conversion of RDS into slowly digested starch (SDS) and resistant starch (RS) during food processing through physical and chemical modifications. Among them, adding external foods or nutrients that conform to dietary habits has attracted increasing attention by reason of its high security and consumer acceptability. Krishnan et al. (2020) added extracted phenolics from pigmented black/red rice to white rice and reported a decreased values related to glycemic response. The individual fatty acids (FAs) were also considered as an effective strategy by binding into the helix structures of amylose/amylopectin molecular chain through hydrophobic effect to form V-type RS (Kawai et al., 2012; Zabar et al., 2009). The ability of V-type inclusion complex to retard the enzyme susceptivity depends on several factors such as aliphatic chain properties, unsaturation degree and composition of the fatty acid (Wang et al., 2016). Many researches have focused on applying pure starch, protein, and individual FAs for simplicity instead of intact grains and edible oil to investigate the mechanism of changes in rice starch digestibility. Also, the interactions between digestibility characteristic and lipid-modified starch were always ignored and may not yet been fully studied.

Starch digestion is a complex process, which is affected by the interaction of a series of factors, including starch granule size, particle morphology, amylose content, starch crystal type, etc (Wang et al., 2020). Diffusion of amylase into the matrix is an important step in enzymatic digestion. The particle size and specific surface area of

starch also play an important role in the enzymatic hydrolysis of starch. With the continuous deepening of the research on the structure of starch granules, different scale levels such as particle structure (granules, 2-10 μm), growth ring structure (growth rings, 120-150 nm), layered structure (amorphous and crystalline lamellae, 9-10 nm), crystalline structure (crystalline, 5-6 nm), and molecular chain structure (crystalline, 5-6 nm) and molecular chain (0.1-1 nm) were formed (Sun et al., 2021). Lindeboom et al., (2004) reported that wheat starch granules with small particles hydrolyzed more rapidly than large granules. The lower sensitivity of macrogranular starches to enzymatic hydrolysis is thought to be due to their smaller granular specific surface area, which may reduce the degree of enzymatic binding and ultimately lead to a lower degree of enzymatic hydrolysis than small granules. The crystal type of starch also significantly affects the digestibility of starch. In general, A-type crystals are more sensitive to enzymatic hydrolysis than B-type crystals due to the different double helix structures of starch granules. The shorter double helix and internal microcrystals in A-type starch granules are more easily digestible (Zhang et al., 2006). Starch digestibility is also related to the chain length of amylopectin, and some studies have shown that the degree of polymerization (DP) 8-12 of amylopectin unit is positively correlated with the enzymatic hydrolysis of starch, while DP16-26 is negatively correlated with the enzymatic hydrolysis of starch (Srichuwong et al., 2005). The longer chains form a longer and more stable helical structure, which is further stabilized by hydrogen bonding, distributed throughout the crystallization region, resulting in a decrease in digestibility (Zabar et al., 2009).

At the same time, the interaction of starch with polyphenols, proteins, and other food components can delay the contact and adsorption of enzymes (Xiang et al., 2023). Lipids, as aggregates of triacylglycerols and micronutrients, were widely applied for household and industrial processing of starchy-based food, including pre-frying (risotto in Italy; paella in Spain), immersion (pilaf in Asia), and frying (fried rice in Asia) (Paesani and Gómez, 2021). Previous studies demonstrated that addition of lipids could decrease the glycemic response of rice grains by forming an inclusion complex with rice starch (Luangsakul and Ritudomphol, 2018a; Farooq et al., 2018). Nevertheless, existing studies have been conflicting as to whether lipids resist lipid-starch complexes formation or assist it. Okumus et al. (2018) investigated the effect of different kind of FAs and lipids (10%, w/w) on cooked starch digestibility and found that the enhanced conversion fractions of RS were

possessed as follows: hydrogenated sunflower oil > palmitic acid > soy oil > stearic acid > corn oil > olive oil. Krishnan et al. (2020b) reported that unsaturated fatty acid (UFA) rich oil has a tendency towards high complexing index favoring the formation of amylose-lipid inclusion complexes. In contrast, Chen et al., (2017) demonstrated that corn starch could not form complexes with corn oil. Absence of V-type complex between starch and edible oil were also reported by Zhao et al., (2023) and Wang et al., (2020). This phenomenon could be attributed to the large steric hindrance effect during complexes formation process due to the large molecular size and complicated structure of lipids or triacylglycerols (Zhao et al., 2022b). Besides, lipids contain multiple nutritional elements, such as phenolic, flavonoid, tocopherol (i.e., β-, γ-, δ-), squalene, γ-oryzanol, β-sitosterol etc., which might inhibit the activities of digestive enzymes. In addition, these compounds might also bind with starch by hydrophobic interactions, hydrogen binding or other molecular forces to form dense structures which could act as physical barriers, and subsequently alter the hydrolysis rate and physicochemical properties of starch (Chi et al., 2019). Moreover, different modification characteristics of starch were reported between lipids and FAs. Okumus et al. (2018) investigated viscosity characteristics and found out that only the oil-modified starch showed a decreased final viscosity, whereas no such phenomenon was observed in the FA modified sample. Lipid coating on starch surface also contributed to physical barriers between digestive enzymes and starch (Paesani and Gómez, 2021) which can be influenced by both the type of lipids and the emulsification speed in intestinal environment. However, only few investigations on such digestive process were carried out, especially of lipid-starch complexes. Meanwhile, unlike the addition of FA, the heat-mass transfer during cooking process could also be influenced by the presence of oil, which could affect the structure and physicochemical properties of starch, thereby affecting the quality of starchy food products (Krishnan et al., 2020). Based on previous researches, the digestibility of oil-modified starch was generally related to the inhibited enzyme activity and physical barrier effects from granular or molecular structure, which mainly influenced by dense gel structure processes and presence of other food ingredients (Paesani and Gómez, 2021). Furthermore, based on those results, we hypothesized that the shell architecture of modified rice granular during mass transfer and heat transfer process in oil-water system could slow down the entry of enzymes, at the same time, the distributed lipids also could prevent enzyme approaches and interaction. The

hypothesis could mean that compared to treatment methods, temperature changes during the treatment process must be considered as an important factor, however, detailed monitoring of temperature rise programs were sometimes lacking.

Wasabi and red chili peppers are not only the commonly consumed seasoning in the cooking process but can also serve as health-promoting substitutes because of their rich content of nutritional compounds and antioxidant activities (Li et al., 2023). As members of the Brassicaceae family, wasabi contains specific bioactive compounds known as glucosinolates, which can interact with myrosinase (EC 3.2.1.147) to form thiocyanates, nitriles, isothiocyanates, and other minor compounds that can act against Escherichia coli (Torrijos et al., 2023). Besides its antifungal compounds, wasabi also contains phenolic acids and flavonoids (Torrijos et al., 2023). Chili peppers contain a rich concentration of bioactive components, including polyphenols, vitamin C, carotenoids, tocopherols, and dietary fiber (Bogusz et al., 2018; Ye et al., 2022). It is noteworthy that chili peppers contain special compounds that give them distinctive flavors called capsaicinoids and have also been shown in medical and health research to have antioxidant, blood glucose control, and anti-inflammatory advantages (Bogusz et al., 2018). Although chili pepper and wasabi have been studied for their epidemiological and health advantages, the effect on the susceptibility of starch to enzymatic hydrolysis in their presence has not been thoroughly investigated. Thus, few reports have concerned the related mechanism, including the release of bioactive compounds during the co-digestion process and the structural changes of starch in the presence of various supplements.

1.2 Objectives

1) To study the impacts of supplements addition conditions on various physicochemical and textural properties of cooked rice.
2) To evaluate the effects of supplements addition conditions on the alteration of resistant starch content in cooked rice.
3) To investigate the effects of supplements addition conditions on *in vitro* starch digestibility of cooked rice.

1.3 Scopes

1) This study is conducted on 3 kinds of supplements.
2) This study is conducted on 2 kinds of addition methods.
3) *In vitro* gastro small-intestinal digestion technique was applied to study starch digestibility.

CHAPTER 2

Effects of adding various supplements on physicochemical properties and starch digestibility of cooked rice

2.1. Introduction

Rice is one of the most important agricultural products due to its high starch content and has been extensively studied as an energy source for humans (Kaur et al., 2016). The structure of starch granules, such as granule size, pores and channels on the granule surface, crystalline shape of the granules, the ratio of straight-chain to branched-chain starch, and the proteins and lipids on the surface affect the digestibility of starch by enzymes (Cervantes-Ramírez et al., 2020).

Oil-modified starch, categorized as resistant starch 5 (RS_5), was a new type of modified starch primarily formed through hydrophobic interaction (He et al., 2020). Based on previous studies, a more order single helical structure could form between lipid molecules and amylose cavity, resulting in starch digestion rate variations (Cervantes-Ramírez et al., 2020). Krishnan et al. (2020) reported that cooked rice supplemented with rice bran oil showed the highest resistant starch content and the lowest in vitro digestion hydrolysis rate, the interactions between fatty acids and alcohols present in the lipids were also confirmed by FTIR spectral fingerprint spectrum within the 950 to 1200 cm^{-1} region. However, the information about the interactions between lipids and starch is limited, indicating that this been research topic has not been thoroughly explored.

Proteins contain many hydrophilic groups, such as carboxyl, hydroxyl, amide, and thiol in alkyl side chains, enabling them to interact with starch molecules (Kumar et al., 2017). For example, Indica rice starch exhibits hydrophobic molecular interactions with soy protein/whey protein isolate and demonstrates hydrophobic, hydrogen bonding, and electrostatic interactions with casein. Thermal treatment further enhanced the formation of a three-dimensional gel network on a micron scale,

which significantly influenced the microstructure of the complexes (Wang et al., 2021). The physicochemical properties and digestion rate were also affected by polyphenols binding to starch through hydrogen bonds and hydrophobic interactions. These interactions may vary depending on the types and concentrations of both polyphenols and starch (Quek and Henry, 2015). Amoako and Awika (2019) reported the resistant starch content increased when proanthocyanidins from high-tannin sorghum were complexed with potato starch due to the formation of type II intrahelical V-complexes. Tea polyphenols have also been demonstrated to decrease the onset temperature (To), peak temperature (Tp), and conclusion temperature (Tc) of rice starch, whereas caffeic acid showed no impact on these parameters (Igoumenidis et al., 2018; Wu et al., 2009).

Wasabi and red chili peppers are popular seasonings in cooking but serve as health-promoting substitutes due to their high levels of nutritional compounds and antioxidant properties (Kurata et al., 2019; Dos Santos Szewczyk et al., 2023). They also contain rich nutritional components, including polyphenols, protein, vitamin C, dietary fiber, and flavonoids (Takahashi et al., 2013; Bogusz et al., 2018; Ye et al., 2022). Their epidemiological and health advantages have thus been studied. However, their mechanism of influence on the susceptibility of starch to enzymatic hydrolysis by digestion in their presence remains insufficiently studied.

In the present study, rice starch complexes with different supplements were prepared to investigate the related mechanism of various guest molecules on starch hydrolysis. All samples were analyzed by multiple analysis techniques in terms of chemical composition and structure. The content of RSD, SDS, and RS during starch hydrolysis and digestion kinetics behaviors were also investigated. Finally, the related mechanism of rice digestibility properties through interaction between starch and chemical composition released from supplements was revealed from the perspective of structural and hydrolysis changes. Our work might provide insight into the starch–supplement interactions and the key factors affecting starch digestibility.

2.2 Materials and methods

2.2.1 Materials and chemical reagents

White rice (Oryza sativa L. cv. Koshihikari, Japan), rapeseed oil, dried chili pepper, and wasabi were purchased from local supermarkets (Matsudo, Chiba, Japan). The glucose assay kit was purchased from Megazyme International Ireland Ltd. (Wicklow, Ireland). Pancreatin (hog pancreas, activity 8 × USP), pepsin (porcine gastric mucosal, ≥ 250 mg^{-1} solid), and invertase (grade VII, ≥ 300 mg^{-1} solid) were purchased from Sigma-Aldrich Co., Ltd. (St. Louis). All other analytical grade reagents were purchased from Dojin Chemical Laboratory Co. Ltd. (Tokyo, Japan).

2.2.2 Sample preparation

All chosen supplements were based on the common eating habits in Asia. Rice grains (400 g) were soaked in 600 mL deionized water for 3 min before cooking in a rice cooker (TK-RC12, Eupa, Tokyo, Japan) according to the Japanese style. 5g rapeseed oil, dried chili pepper, and wasabi were mixed with cooked rice. The resulting samples were designated as follows: cooked rice with added rapeseed oil (RRS), cooked rice with added dried chili pepper powder (CRS), and cooked rice with added dried wasabi powder (WRS). Rice cooked without any added additives was designated as the control group (CT). All samples were placed in petri dishes and covered with plastic wrap to allow moisture equilibration in an incubator set at 35°C for 25 minutes. The in vitro digestibility was determined instantly after equilibrium. Meanwhile, the measurement of moisture, color, and texture was completed within 20 min. The remaining samples were stored overnight in a -80 °C refrigerator and then freeze-dried. The obtained samples were ground into powder and passed through a 200-sieve mesh. The sealed rice flour was stored in a sealed bag at 4 °C for further analysis.

2.2.3 Moisture content

Approximately 5.0 ± 0.2 g of cooked grains and 3.0 ± 0.2 g of sealed rice powder

were dried at 135 °C for 36 h in an air oven (Oven 8150, Labserv, Longford, Ireland) according to Tamura et al. (2023), and the moisture content (% w.b.) was calculated as the weight loss (%) difference before and after drying using the following formula:

$$\text{Moisture content (\%)} = (W_2 - W_1)/W_2 \times 100$$

where W_2 and W_1 are the weight of the sample before and after drying, respectively.

2.2.4 Crude protein (CP) content

The nitrogen content of the powdered sample (0.15 g) was determined using a CN Coder (MT-700, Yanaco, Kyoto, Japan). A nitrogen– protein conversion factor (5.95) was used to calculate the crude protein content based on the nitrogen content results. Hippuric acid (200-37032) was purchased from Kishida Chemical (Osaka, Japan) and was used as the standard nitrogen material (Tamura et al., 2021).

2.2.5 Texture analysis

A creep meter (RE2-3305S, Yamaden Co. Ltd., Tokyo, Japan) equipped with a 20 N load cell was used to determine the texture characteristics of cooked samples. The compression test mode was defined as the surface (25% of initial thickness) and overall (90% of initial thickness) when measuring firmness and adhesiveness. A single cooked grain was placed on a cylindrical baseplate and compressed twice using a planar plunger (Ø56 mm) at a speed of 1 mm/s with the contact point between the plunger and grain set as 0.02 N trigger force. Two positive curves (surface firmness and overall firmness) and two negative curves (surface and overall adhesiveness) for the texture profile were obtained (Tamura et al., 2019). The thickness of the sample was recorded as the distance between the plunger and baseplate. Approximately 15 replicates were completed within 20 min to maintain the moisture and textural properties during testing.

2.2.6 Simulated in vitro gastro-small intestinal digestion

The total starch (TS) contents of the powdered rice flour were measured according to the total starch assay kit (K-TSTA 07/11, Megazyme International,

Wicklow, Ireland) based on AOAC Method 996.11 and AACC Method 76–13.01. Simulated gastric fluid (SGF) and simulated intestinal fluid (SIF) were prepared according to a previously reported method (Dartois et al., 2010). A magnetic stirrer (color squid white, IKA, Staufen, Germany) was used to continuously agitate the sample (200 rpm) in the reactor. Cooked rice grains were placed into a net bag and then placed in a jacketed glass reactor at 37 °C. Then, 170 g of 4% TS equivalent cooked rice grains were subjected on a two-stage simulated gastro-intestinal in vitro digestion model (Tamura et al., 2016a). The experimental conditions have been described by Dartois et al. (2010) and Tamura et al. (2016). The pH of gastric digestion was adjusted to 1.20 ± 0.02 with 6 M HCl at the initial gastric phase (G0) and then with 1 M HCl at subsequent stages (G15, G30). The digestive solution (0.5 mL) was collected at 5, 15, and 30 min. After 30 min of gastric digestion, 23 mL of SIF was added to simulate intestinal digestion, and the pH was maintained at 6.80 ± 0.02 with 3 N NaOH and 1 N NaOH. The digestive solution (0.5 mL) of the small intestinal digestion phase was collected at 5, 15, 20, 30, 60, 90, 120, 180, 240, 300, 360, and 480 min. All collected digestive solutions were adjusted to a tube, and the digestive enzyme was terminated by mixing thoroughly with 3 mL of 95% ethanol. The collected samples were centrifuged (1800×g, 10 min) and incubated with amyloglucosidase and invertase at 37 °C for 10 min. The glucose concentration was measured using a D-glucose assay kit (GOPOD, Megazyme International Ireland). The results of starch hydrolysis were calculated as percentage (%) following the equation:

$$\%S_H = S_h/S_i = 0.9 \times G_p/S_i$$

where $\%S_H$ is the percentage of starch hydrolysis, S_h, S_i and G_p are the amount of hydrolyzed starch, initial TS, and the glucose produced, respectively. A conversion factor of 0.9 was used, which is calculated from the molecular weight of the starch monomer against that of glucose (162/180= 0.9) (Goñi et al., 1997).

The content of the starch fraction (RDS, SDS and RS) based on %SH was calculated as follows:

$$\mathrm{RDS}(\%) = \mathrm{C_{I20}} - \mathrm{C_{G30}}$$

$$\mathrm{SDS}(\%) = \mathrm{C_{I120}} - \mathrm{C_{I20}}$$

$$\mathrm{RS}(\%) = 100 - \mathrm{C_{I120}}$$

where C_{G30} is the percentage of hydrolyzed starch at 30 min of gastric digestion, C_{I20} and C_{I120} are the percentages of hydrolyzed starch at 20 and 120 min of small intestinal digestion.

2.2.7 Dynamic analysis of in vitro enzymatic hydrolysis

A non-linear first-order equation model was applied to calculate the kinetics of starch hydrolysis as described below (Goñi et al., 1997):

$$\mathrm{C} = \mathrm{C_\infty}\left(1 - \exp^{-\mathrm{kt}}\right)$$

where C and C_∞ represent the hydrolysis percentage at digestion time t and the equilibrium percentage of starch during the simulated intestinal digestion phase, respectively, and k is the kinetic constant.

The fitting quality of the first-order equation model was evaluated using the determination coefficient (R^2).

$$R^2 = 1 - \frac{\sum_{\mathrm{i}=1}^{N} (C_{exp,\,\mathrm{i}} - C_{pre,\,\mathrm{i}})^2}{\sum_{\mathrm{i}=1}^{N} (C_{exp,\,\mathrm{i}} - C_{ave})^2}$$

where $C_{exp,\ i}$ and $C_{pre,\ i}$ represent the experimental and predicted percentages of hydrolyzed starch from the "i"-th experiment, respectively. Cave is the average experimental percentage of hydrolyzed starch, and N represents the number of observations.

The hydrolysis index (HI) was defined as the area of the hydrolysis curve of cooked grain samples divided by that of white bread. The estimated glycemic index (eGI) was calculated using the formula from (Goñi et al., 1997):

$$\mathrm{eGI} = 39.71 + 0.549\mathrm{HI}$$

2.2.8 Statistical analysis

Statistical data and differences in at least triplicate measurements were calculated as means ± standard deviations, and analysis was conducted using the t-test (IBM

SPSS Statistics, version 25.0; IBM Corp., Armonk, NY, USA). A priori significance level of $p < 0.05$ was identified statistically significant with an analysis of variance (ANOVA).

2.3 Results and discussion

2.3.1 Textural properties

The firmness, adhesiveness, and thickness of cooked rice grains mixed with different supplements are shown in Table 2.1. The cooked rice without adding anything had the lowest surface firmness (SF) compared to others, whereas the SF of rice grains increased with the presence of additives ($p < 0.05$). Under high temperature and moisture conditions during cooking, rice grains might form cracks on the surface due to water absorption and expansion of starch granules (Tamura et al., 2021). These cracks facilitate the entry of water molecules into the starch, promoting further starch gelatinization (Thuengtung et al., 2021). In addition, a decreased gelatinization enthalpy was reported as polyphenols, proteins, and other nutritional ingredients added, The interaction through hydrogen bonds, hydrophobic interactions, or other molecular forces may result in the attachment of these molecules to the grain surface, forming a gel network that can alter the firmness, adhesiveness, and digestibility of the starch (Han et al., 2020). Zhao et al. (2023) added oil into tapioca starch and compared the gel network with native starch after heat treatment, the physical entanglements of starch molecular chains were strengthened and the firmness of three-dimensional gel network was promoted, inhibiting the swelling of starch. This phenomenon was also supported by the lower thickness of RRS (2.23 ± 0.10 mm) compared with CT (2.23 ± 0.10 mm). The effect of caffeic acid on maize starch was evaluated by Zheng et al. (2020) and found that caffeic acid improved the solubility and swelling power of the sample compared with native maize starch. Compared with CRS (0.80 ± 0.14 N) and WRS (0.77 ± 0.03 N), the SF of RRS increased significantly to 0.95 ± 0.08 N, which can be explained mainly by water evaporation during the equilibrium period. Water migration from inside to outside was further promoted by the low moisture content of the dried chili pepper powder and dried wasabi, resulting in a quick moisture loss on the surface of the rice grains, which might contribute to a higher SF. The effect of moisture transfer on SF was demonstrated by Tamura et al.

(2019). They found out that rice grains stored at 90 °C have a harder surface than grains stored at 30 °C, which was considered as continuous and quicker water transfer from inside core to drying surface layers; thus, a higher SF was observed, which was consistent with our results. Simultaneously, the evaporation of water, swollen space architecture of starch granules, and capillary pressure difference provided more space for oil absorption (D. Yang et al., 2019). The oil absorption phenomenon was reported by Wu et al. (2024), who quantified the oil distribution between tigernut starch and tigernut oil by CLSM image. The matrix oil adsorption value was reported to increase from 1.10 g/100 g to 1.83/100 g with temperature increasing from 80 °C to 140 °C, which is related to the heat-induced pressure difference between starch and oil. Zhao et al. (2023) also indicated that after adding oil to tapioca starch, not only a well-linked gel network structure was constructed but also the disrupted starch gel network was partly reversed by oil modification, which could be explained by the higher SF of RRS in our current study. However, the change in overall firmness (OF) showed the opposite trend to the surface firmness. Harder cores of rice grains were observed in CRS (18.14 ± 1.53 N) and WRS (17.88 ± 0.91 N), which might be related to continuous water migration from the rice grain to the powder. In contrast, RRS (15.02 ± 1.11 N) showed a significantly softer core compared to CT (16.43 ± 2.08 N), which could be associated with the triglycerides in oil, which could form a lipid-enriched phase as a physical barrier, retaining the moisture within the grains, thus resulting in a soft core (Li et al., 2020; Wang et al., 2019). For the surface adhesiveness (SA), a slight decrease in CRS and WRS was considered to be connected with the physical barrier effect of the dried chili pepper powder and dried wasabi powder. The RRS showed the lowest SA ($1.43 \pm 0.25 \times 10^{-2}$ N), which could be explained by the formation of the lipid-enriched phase. Compared with the incompleteness of powder coating, oil provides complete coverage on the surface of rice grains and completely blocks the viscosity of starch due to its fluidity (P. Li et al., 2020). Previous study reported similar findings by Paesani and Gómez (2021) where the surface adhesiveness (SA) of rice grains decreased significantly after pre-frying with oil. However, the authors did not find any correlation between adhesiveness and damaged starch, indicating that the reduction in SA was solely attributed to the presence of oil in the surface layer rather than alterations in the starch itself. Overall adhesiveness (OA) was found to be not significantly different with the lowest OA

showing in RRS (2.33 ± 0.29 N) as well. The changes in OA and SA were considered due to the physical barrier of the supplements.

Table 2.1. The texture characteristic of cooked rice grains with addition of different supplements.

Sample	Firmness		Adhesiveness		Thickness (mm)
	Surface (N)	Overall (N)	Surface (10^{-2} N)	Overall (N)	
CT	0.74±0.11 a	16.43±2.08 ab	8.43±0.47 d	3.91±0.71 c	3.33±0.28 a
RRS	0.95±0.08 b	15.02±1.11 a	1.43±0.25 a	2.33±0.29 a	2.23±0.10 a
CRS	0.80±0.14 ab	18.14±1.53 b	6.55±0.38 b	3.33±0.48 bc	2.35±0.07 a
WRS	0.77±0.03 ab	17.88±0.91ab	7.22±0.11 c	2.93±0.20 ab	2.30±0.14 a

CT, cooked rice; RRS, cooked rice added with rapeseed oil; CRS, cooked rice added with dried chili pepper powder; WRS, cooked rice added with dried wasabi powder. All data are expressed as averages measurements with standard deviation. The sample number (n) is 4-5. Different lower-case letters in the same column indicate significant differences ($p < 0.05$).

2.3.2 Moisture content

The moisture content (MC%) is summarized in Table 2.2. The cooked rice grain with dried wasabi and red chili pepper powder showed lower moisture content (48.22 ± 1.18% w.b. and 48.49 ± 1.00% w.b.) than the control (54.90 ± 0.85% w.b.). The decrease in MC% might be attributed to the lower MC% of dried wasabi and red chili pepper powder. In contrast, rice grains added with oil showed the least reduction of MC% (52.63 ± 1.06% w.b.), which was likely due to the surface lipid layers affecting the evaporation of water (Zhao et al., 2023).

Table 2.2 The effect of different supplements on the moisture, CP, RDS, SDS and RS contents for cooked rice grains.

Sample	CP (% d.b.)	Moisture content (% w.b.)	RDS (%)	SDS (%)	RS (%)
CT	6.83±0.02 b	54.90±0.85 c	11.59±0.01 c	35.85±0.45 c	52.56±0.44 a
RRS	6.40±0.03 a	52.63±1.06 b	9.11±0.87 a	31.27±0.41 a	59.62±0.46 c
CRS	7.58±0.03 c	48.49±1.00 a	9.31±0.05 a	33.40±0.28 b	57.29±0.34 b
WRS	8.10±0.02 d	48.22±1.18 a	10.76±0.14 b	36.39±0.19 c	52.85±0.33 a

CP: crude protein; RDS: rapidly digested starch; SDS: slowly digested starch; RS: resistant

starch. The sample number (n) was as follows: CP (n = 4-6); moisture (n = 4-6); RDS, SDS and RS (n = 3-4).

2.3.3 Crude protein (CP) content

The CP of cooked rice grains with the addition of different supplements is expressed in Table 2.2. The CP content of CT was 6.83% db, which is similar to the variety of Kirara 397 (Oryza sativa L.) (7.93 % d.b.) reported in a previous study (Tamura et al., 2023). The difference between these two samples might be related to the variety, cultivation environment, and cooking method. The CP content of other samples ranged from 6.40% db to 8.10% db, which was significantly influenced by the different additions of supplements. RRS showed the lowest CP content, whereas WRS showed the highest CP content. Similar results were reported by Tamura et al. (2023) that rice cooked with rapeseed oil had a lower CP content of 7.70 % db than the control group (7.93 % d.b.) owing to the low CP content in rapeseed oil as well as the breaking down of proteins into nitrogen-containing aroma compounds (Yang et al., 2008). Meanwhile, the CP content of CRS and WRS was significantly increased by the addition of dried chili pepper powder and dried wasabi powder. The reason might be that proteins are one of the main biomolecules found in seed material (Tamura et al., 2021). Le Gall et al. (2021) summarized 36 types of wasabis and found that the protein composition ranged from 22.3 %DM to 29.7 %DM depending on the variety. Changes in protein content from chili powder are also contributed by various factors such as drying treatments, raw materials, and processing methods (Ye et al., 2022).

2.3.4 Starch hydrolysis during in vitro gastro-small intestinal digestion

The hydrolysis of cooked rice starch with different supplements is measured as shown in Fig. 2.1. Starch digestibility can be influenced by many factors, including starch sources, molecular structure, crystallinity, and modification (Srichuwong et al., 2007). Almost no hydrolysis phenomenon was exhibited during simulated gastric digestion, consistent with previous research (Tamura et al., 2019). This might be due

to the lack of enzymes for starch hydrolysis in the simulated gastric fluid. Similar results were observed by Tamura et al. (2022). However, it was considered that the physical properties of starch and supplements could be altered by the digestive environment of the stomach (Xiang et al., 2023). All rice samples exhibited a decreased digestion pattern compared with CT during the simulated small intestine digestion process, which might be related to the interaction between starch and various guest molecules. Krishnan et al. (2020b) reported that the accessibility of enzymes to starch might be reduced by matrix compounds such as protein, lipids, and phenolics, thus affecting starch digestibility. Farooq et al. (2018) elucidated the formation of amylose-lipid complexes during rice cooking with palm oil and observed an increase at a peak of 20° 2θ which representing V-type complexes. Meanwhile, the increased melting enthalpy and resistance starch content also contributed to the reduced in vitro starch digestibility. Additionally, Zhao et al. (2022) reported complete disintegration of natural starch while starch added with oil maintained a granular shape, suggesting that the starch structure could be reinforced by cross-linked bonds between oil. Previous studies reported that the oil-enriched phase on rice grains could cause agglomeration and adhesion of starch granules due to hydrophobic lipids, enabling the starch gel network on the surface to be more stable, restricting further leaching of amylose and approaching digestive enzymes, thus decreasing starch digestibility (Cervantes-Ramírez et al., 2020). Similar results were observed in our experiment in which a reduction of starch digestibility was shown in RRS (80.42%) compared with CT (86.66%). It is worth noting that RRS showed a lower degree of starch hydrolysis than CRS and WRS at the small intestine stage until 180 min, which might be due to the intact starch granule forms and the surface lipid layers. In addition, the higher starch hydrolysis degree is probably due to the emulsification of oil in digestive juices, which reduces the physical barrier effect to enzymes (Xiang et al., 2023). Promoted digestive degradation of lipids was reported by Xiang et al. (2023) that bile salts as natural surfactants (Na^+, K^+, and PO_4^+) suggested easier exposure of starch encapsulated in lipids. In contrast, the higher enzyme resistance of CRS and WRS in the later stages (I 180 min-I 420 min) may be due to the release of phenolic

compounds. Previous report quantified the impact of phenolics on rice starch digestion by incorporating phenolics extracted from pigmented brown rice and red rice into white rice Krishnan et al. (2020a)found a reduction in starch hydrolysis ranging from 9.2% to 10.7%, highlighting phenolics as significant matrix compounds that contribute to lowering the glycemic response. The relationship between polyphenols and lower rates of digestion was also reported by Quek and Henry (2015), who determined the effects of lingonberry, cranberry, and red grape on white rice, while a significant reduction of glucose release level was observed after the addition of red grape. Meanwhile, as the concentration of red grape polyphenols increased, the digestibility of white rice decreased with a positive correlation ($R = 0.9854$), which shows that phenolics might be a critical factor in regulating glycemic response. Similar roles of polyphenols in modulating the in vitro digestibility of starch have also been reported from various berry sources (Zheng et al., 2021).

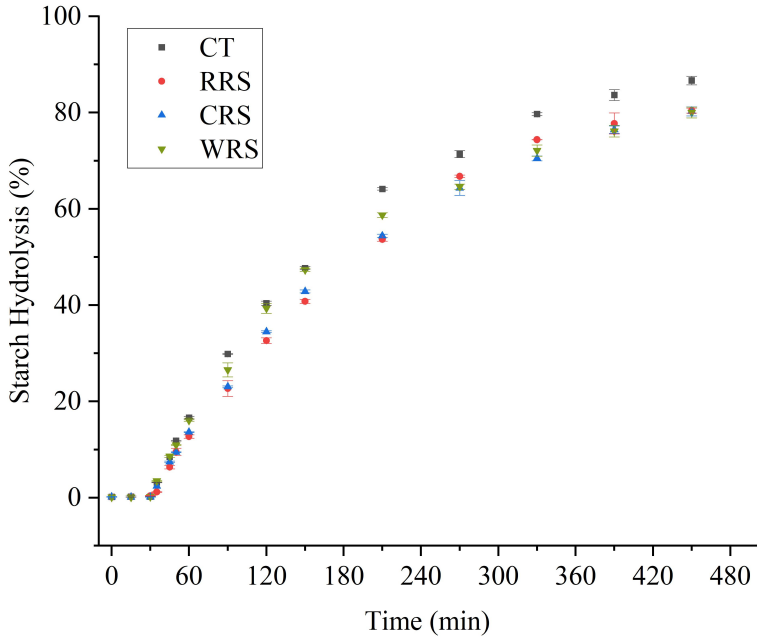

Fig. 2.1. Changes in starch hydrolysis (%) of intact cooked rice grains adding various supplements. Error bars represent standard deviation (n = 3-6).
CT: cooked rice; RRS: cooked rice adding rapeseed oil; CRS: cooked rice adding dried chili pepper powder; WRS: cooked rice adding dried wasabi powder.

2.3.5 Resistant starch (RS) content

To further reveal the glycemic potential of different samples, three nutritional variants of starch (RDS, SDS and RS) were calculated (Table 2.2.). CT was rapidly digested, with most of the starch being hydrolyzed during the small intestine stage, leading to the highest RDS and SDS values of 11.59% and 35.85%, respectively. The RDS (9.11%) and SDS (31.27%) in RRS were much lower than those in CT, while the RS (59.62%) were much higher, indicating that some of the SDS and RDS in native starch were converted into RS after oil addition. Similar transformations were observed by Farooq et al. (2018) in white rice starch, in which RDS and SDS decreased from 71.20% and 9.80% to 69.90% and 8.40%, respectively, while RS increased from 18.90% to 23.90% after coking with palm oil. CRS and WRS also showed significant reduction in the RDS content (9.31% and 10.76%) compared with CT. Previous research reported that the RDS content reduced from 67.68% to 45.64%, while the RS content increased from 13.29% to 36.29% as the binding contents between rice starch and proanthocyanidins extracted from Chinese berry leaves increased, indicating that the combination with proanthocyanidins was beneficial to the conversion of starch to RS, as well as the inhibition of digestive enzymes by the released proanthocyanidins during digestion site trend of SDS and RS in CRS and WRS were observed compared with CT (Zheng et al., 2021). This difference in starch type can be attributed to the different sources and release speeds of nutrient substances inside the supplements and the interaction between starch and starch granule morphology (Chi et al., 2018; M. Li et al., 2020).

2.3.6 Kinetics of starch digestibility

The kinetic parameters for evaluating differences during small intestinal digestion associated with hydrolysis calculated by a non-linear fitting method to a first-order equation model are summarized in Table 2.3. All kinetic parameters were significantly affected by the addition of different supplements. RRS showed higher C_∞ of 94.92%, while k was the lowest among all samples, which might be related to lower

digestibility in the prophase of the small intestine due to the physical barrier of oil and reinforced structure by cross-linking (Zhao et al., 2023). The CRS and WRS had the lower C_∞ of 89.64 and 83.49%, respectively, while the CRS showed a higher k (0.68) than WRS (0.53), suggesting that starch digestibility could be affected by the sources and release rates of phenols and other nutrients (M. Li et al., 2020). All first-order equation models exhibited high R^2, suggesting that starch hydrolysis was well described. eGI was determined to simulate the level of glucose release. All samples showed significantly lower eGI compared with CT, suggesting that the addition of lipids and phenols in carbohydrate-rich foods might be a practical means to reduce the glycemic response of starchy food eaten worldly.

Table 2.3. The kinetic parameters of starch hydrolysis of rice grains cooked with lipids under various conditions.

Sample	C∞ (%)	$k \times 10^{-2}$ (min^{-1})	R^2	HI	eGI
CT	93.35±1.55 c	0.63±0.02 c	0.99	68.80±0.57 c	77.48±0.31 c
RRS	94.92±2.28 c	0.48±0.02 a	0.99	61.05±0.85 a	73.23±0.46 a
CRS	89.64±1.54 b	0.53±0.02 b	0.99	60.76±0.57 a	73.07±0.31 a
WRS	83.49±1.69 a	0.68±0.03 d	0.99	63.65±0.63 b	74.65±0.34 b

Mean ± standard deviation. The sample number (n): C∞ (n = 3-6); k (n = 3-6); HI (n = 3-6); eGI (n = 3-6). Different letters within the same column indicate significant differences ($p < 0.05$).

2.4 Conclusions

In the present study, the rice starch complexes with different supplements were prepared and the physicochemical and digestive characteristics were determined. All samples added with supplements had increased SF and decreased thickness, which was attributed to the swelling and gelatinization affected by lipids layer and

combination with guest molecules as well as migration of water content. Starch hydrolysis kinetic parameters of C_∞, k and eGI of the samples were influenced by supplements significantly. Cooked rice grain with the addition of rapeseed oil showed the highest RS content while CRS also exhibited a higher RS content and lower SDS content during in vitro digestion. The higher resistance to hydrolytic enzymes of samples were considered as the combination of the physical barriers formed by lipids and polyphenol and effects of the inhibition of enzymes by released nutrients. In general, the addition of rapeseed oil and dried chili pepper powder might be considered as a potential way to increase the proportion of RS and reduced the enzymatic hydrolysis during digestion. Because this study investigated different supplements on physicochemical properties and starch digestibility of cooked rice, the effects of the amount of supplements added and its composition should be addressed in future studies.

CHAPTER 3

Effects of adding various supplements on multiscale structure of cooked rice

3.1 Introduction

The structure of starch granules, such as granule size, pores and channels on the granule surface, crystalline shape of the granules, the ratio of straight-chain to branched-chain starch, and the proteins and lipids on the surface affect the digestibility of starch by enzymes (Cervantes-Ramírez et al., 2020).. Oil-modified starch, categorized as resistant starch 5 (RS_5), was a new type of modified starch primarily formed through hydrophobic interaction (He et al., 2020). Based on previous studies, a more order single helical structure could form between lipid molecules and amylose cavity, resulting in starch digestion rate variations (Cervantes-Ramírez et al., 2020). However, the information about the interactions between lipids and starch is limited, indicating that this been research topic has not been thoroughly explored. A previous study reported that proteins contained many hydrophilic groups such as carboxyl, hydroxyl, amide, and thiol in alkyl side chains, enabling them to interact with starch molecules (Kumar et al., 2017). Indica rice starch exhibited hydrophobic molecular interactions with soy protein/whey protein isolate and demonstrated hydrophobic, hydrogen bonding, and electrostatic interactions with casein. Thermal treatment further enhanced the formation of a three-dimensional gel network on a micron scale, which significantly influenced the microstructure of the complexes (Wang et al., 2021). Furthermore, the physicochemical properties and digestion rate were also affected by polyphenols binding to starch through hydrogen bonds and hydrophobic interactions. These interactions may vary depending on the types and concentrations of both polyphenols and starch (Quek and Henry, 2015). Amoako and Awika, (2019) reported the resistant starch content increased when proanthocyanidins from from high-tannin sorghum

were complexed with potato starch, due to the formation of the type II intrahelical V-complexes. Tea polyphenols also have been demonstrated to decrease the onset temperature (To), peak temperature (Tp), and conclusion temperature (Tc) of rice starch, whereas caffeic acid showed no impact on these parameters (Igoumenidis et al., 2018; Wu et al., 2009). While chili pepper and wasabi have been studied for their epidemiological and health advantages, their mechanism of influence on the susceptibility of starch to enzymatic hydrolysis by in vitro digestion in their presence remains insufficiently studied.

Thus, the aim of this work is to explore the interactions between starch and various supplements, including rapeseed oil (RRS), dried chili pepper powder (CRS), and dried wasabi powder (WRS), by examining their short-range structures, morphological characteristics, physicochemical properties, and starch hydrolysis. The multi-scale structures and molecular interaction forces of obtained complexes were characterized using combined analytical techniques. Differences in the resistant starch content and digestion kinetics behaviors related to the mechanism of in vitro digestion were also examined. This work might provide a scientific basis for further application of supplements in the formulation of starch-based functional foods.

3.2 Materials and methods

3.2.1. Sample preparation

Rice grains (400 g) were soaked in 600 mL deionized water for 3 min before cooking in a rice cooker (TK-RC12, Eupa, Tokyo, Japan) according to the Japanese style. Rapeseed oil, dried chili pepper, and wasabi (10%, w/w) of dry weight basis were mixed with cooked rice. The obtained samples were donated as RRS, CRS, and WRS. Rice cooked without added items was donated to the control group (CT). All samples were transferred into Petri dishes with a plastic wrap to equilibrate moisture in an incubator at 35 ℃ for 25 min. Subsequently, 40 g of the cooked grains were stored overnight in a -80 ℃ refrigerator and then freeze-dried. The obtained samples were ground into powder and passed through a 200-sieve mesh. The sealed rice flour

was stored in a sealed bag at 4 ℃ for further analysis.

3.2.2. Resistant starch content

The digestion resistant fraction was determined according to AOAC Method, using the RS assay kit (K-RSTAR; Megazyme International Ireland). About 100 mg powder sample was weighed into screw cap tube and incubated with pancreatic α-amylase (10 mg/mL) and AMG (3 U/mL) at 37 ℃ for 16 h. This process aimed to hydrolyze and solubilize non-resistant starch components. Four milliliters of ethanol (99% v/v) was added to terminate the reaction, then the recovered resistant starch by centrifugation and washed with 2 M KOH. Afterwards, 8 mL of 1.2 M sodium acetate buffer (pH 3.8) was added to neutralize the high alkalinity of the obtained solution and AMG was used to quantitatively hydrolyze the resistant starch fraction. The glucose was determined by glucose oxidase/peroxidase (GOPOD) reagent. The contents of RS were calculated as suggested by the manufacturer's protocol.

3.2.3. Fourier transform infrared spectroscopy (FTIR)

To characterize the structural changes induced by supplements in rice starch, the FTIR spectra of freeze-dried powder samples and supplements were recorded using a Fourier transform spectrophotometer (FT/IR-4200ST+ IRT-5000, Jasco Corporation, Japan). The spectra were scanned in the range of 4000 – 400 cm^{-1}. Sixty-four accumulation scans were obtained at a resolution of 2 cm^{-1} (Krishnan et al., 2020).

3.2.4. Morphology and tissue structure

The microstructural changes of grain samples under external and internal conditions were observed using Scanning Electron Microscopy (SEM) (SU1510; Hitachi High-Tech, Tokyo, Japan). The freeze-dried samples were mounted on double-sided adhesive tape and observed in high vacuum mode at an accelerating voltage of 5 kV. The obtained images were analyzed by graphic software (Photoshop, Adobe, San Jose, CA, USA).

3.2.5. Statistical analysis.

Statistical data and differences based on at least triplicate measurements were presented as means ± standard deviations. Analysis was conducted using the t-test (IBM SPSS Statistics, version 25.0; IBM Corp., Armonk, NY, USA), with a priori significance level set at $p < 0.05$ considered statistically significant. The principal component analysis (PCA) was performed using Origin 2018 (Origin Lab, California, USA).

3.3 Results and discussion

3.3.1. Resistant starch (RS) content

To further reveal the glycemic potential of different samples, the resistant starch (RS) content was calculated (Figure 3.1.). After adding supplement, the resistant starch increased in all samples. Similar results were observed by Farooq et al. (2018) in white rice starch, in which RS content increased from 18.90% to 23.90% after coking with palm oil. CRS and WRS showed a higher RS content than RRS, which might be attributed to the easier accessibility of polyphenols while the interaction between starch and fatty acids were obstructed by triglyceride macromolecules and oil-rich layers (Zhao et al., 2023). Previous research reported that the RS content in rice increased from 13.29% to 36.29% as the binding contents of proanthocyanidins (extracted from Chinese berry leaves) increased, indicating that the combination with proanthocyanidins was beneficial to the conversion of starch to RS, meanwhile, digestive enzyme activity was also inhibited by the released proanthocyanidins during digestion (Zheng et al., 2021). The difference in RS content might be attributed to the different sources and release speeds of nutrient substances inside the supplements and the interaction between starch and starch granule morphology (Chi et al., 2018; M. Li et al., 2020).

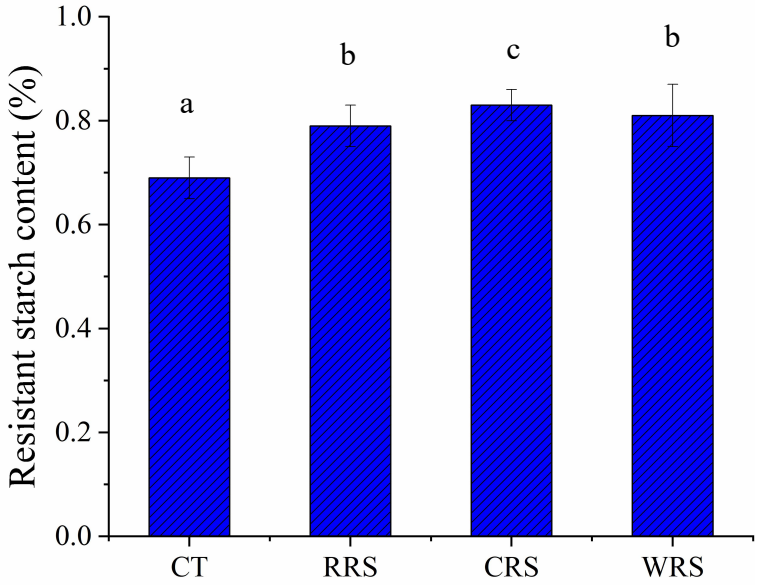

Fig. 3.1. The effect of adding various supplements on the resistant starch (RS) contents of cooked rice grains. Notes: CT: normal cooked rice (control); RRS: cooked rice adding rapeseed oil; CRS: cooked rice adding dried chili pepper powder; WRS: cooked rice adding dried wasabi powder. Mean ± standard deviation.

3.3.2. Short-range ordered structure

FT-IR spectra of cooked rice, complexes as well as supplement alone are presented in Fig. 3.2. Different FTIR spectra was observed among different supplements. High intensity peak around 3016 cm^{-1} were observed in rapeseed oil, which might relate to the unsubstituted polynuclear aromatic C-H stretching. Similar results were reported by Asemani and Rabbani (2020), noting that the spectral range from 3050 to 3000 cm^{-1} was related to the number of rings in aromatic compounds, whereas an opposite trend was detected between the number of rings and wavenumber. Characteristic transmittance peaks were identified around 2860 and 2964 cm^{-1}, ascribed to asymmetric and symmetric stretching vibrations of CH_2 and CH_3 groups in fatty acids, and a peak at 1752 cm^{-1} due to the C=O in saturated esters, as observed in rapeseed oil. In addition, the peaks around 2860 and 1752 cm^{-1} were observed in chili pepper powder and wasabi powder, which might correspond to the lipids retained within the seed. The peaks in the range of 1580-1720 cm^{-1} and 1480-1580 cm^{-1} were assigned as typical protein bands of amide I and amide II, respectively (Y. Li et al., 2024). In the present study, these characteristic peaks were basically the same as those

of complexes cooked, which indicated that covalent interactions did not form during cooking. Yang et al. (2019) reported a similar spectrum when characterizing the interaction between corn starch and whey protein isolate (WPI). They observed strong bands around 1540 cm^{-1} and 1655 cm^{-1} in WPI and all complex samples. Notably, a significant shift to lower wavenumbers in the range of 3700-3000 cm^{-1} were detected in the complexes of CRS and WRS, reflecting an increased hydrogen bond density and strength. These bound hydroxyl groups could be formed between polar residues of protein (serine, aspartic acid, glutamic acid and threonine) and hydroxyl groups of starch, as well as backbone amine and carbonyl groups (Li et al., 2024). Li et al. (2024) reported a similar shift in spectral bounds of pea protein and chestnut starch complexes, from 3313 cm^{-1} to 3274 cm^{-1}, following cooking treatment. This shift was attributed to the lower bond force constant of hydrogen bonds involving combined hydroxyl groups compared to free hydroxyl groups (Lu et al., 2016; Wang et al., 2021). The stretching vibrations for primary and secondary alcoholic groups were shown in the range of 3100-3500 cm^{-1} as well as the skeletal mode vibration in α-(1-4) glycosidic linkage of peak around 937 cm^{-1}, which were common in all complexes and control group. Meanwhile, rice starch also showed IR patterns featuring characteristic transmittance peaks around 990 cm^{-1}, corresponding to the C-O stretching vibrations of C-O-C glycosidic linkages in the polysaccharide. Peaks at 1640-1650 cm^{-1} were attributed to the O-H bonds involved in scissor bending vibration during starch hydration. In addition, two absorption peaks at 2856 and 1748 cm^{-1} were observed in all complexes as well as chili pepper powder and wasabi powder, which were ascribed to the asymmetric and symmetric stretching vibrations of $–CH_3$ and $–CH_2$ in the fatty acids and vibration of carbonyl. New signals at 1683 and 1435 cm^{-1} also appeared in all samples, which could be associated with a possible interaction between starch and polyphenols. Similar spectrum results were observed by Han et al. (2020), where new signals at 1685 and 1447 cm^{-1} appeared in the gallic acid-rice starch complexes while no such peaks were observed in samples of gallic acid or rice starch individually. Compared to the corresponding mixture, the FT-IR spectrum at 1654, 1558, 1547, 1512, 1460, 1385, 1240 and 1160 cm^{-1} had shifted and

diminished, which implied that the interaction between the nutritional compounds and rice starch could prompt the shifting and disappearance of spectrum peaks. In summary, the variations among the FT-IR spectrum indicated that there might be differences among the main interactions between different supplements and rice starch.

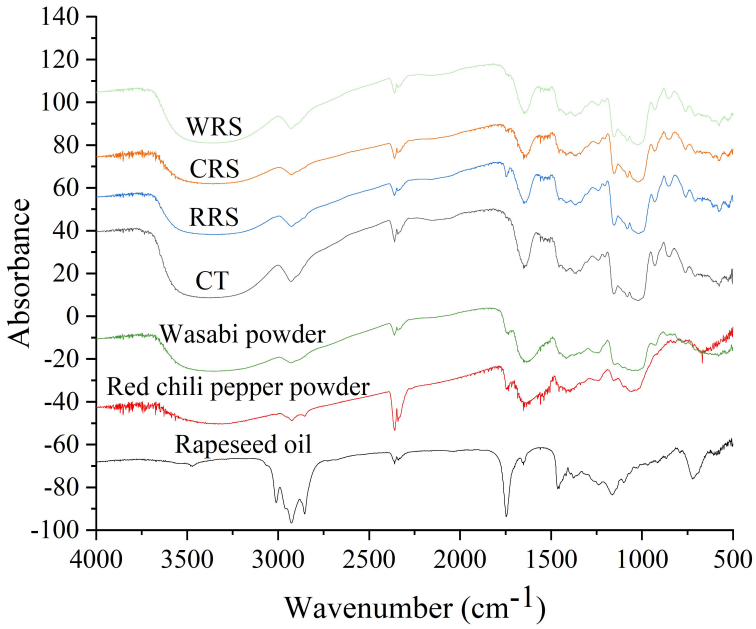

Fig. 3.2. Fourier transform infrared spectroscopy spectra of cooked rice grains with different supplements. Notes: CT: normal cooked rice (control); RRS: cooked rice adding rapeseed oil; CRS: cooked rice adding dried chili pepper powder; WRS: cooked rice adding dried wasabi powder.

3.3.3. Morphology and tissue structure

Scanning electron microscope (SEM) was used to investigate the effects of different supplements on the morphology of cooked rice (Fig. 3.3 and Fig. 3.4). Compared to CT, the cooked rice added with different supplements showed evident morphological differences. The CT samples exhibited relatively smooth spherical shape, alongside dense pore-like structures and cracks on the surface (Fig.3.3a). The SEM images of rice supplemented with rapeseed oil revealed a transparent granular structure with a noticeable oil-enriched surface phase. Additionally, large protrusions and clusters were observed (Fig.3.3b). The results indicated that the leached starch during cooking

process might interact with starch by the lipid crosslinking and agglomeration effect (Ding et al., 2018). Previous studies reported that V-type resistant starch formed by crosslinking bonds between starch and lipids could retard starch digestion due to ordered structure (Zhao et al., 2022; Paesani and Gómez, 2021). Moreover, characteristic agglomeration on CRS (Fig.3.3c) and WRS (Fig.3.3d) were also observed, which might be attributed to the noncovalent interactions with polyphenol and hydrogen bonding with protein among starch components (Wang et al., 2021; Han et al., 2020). Yang et al. (2019) reported reduced starch digestibility and an ordered structure where whey protein aligned in parallel with corn starch through hydrogen bonds. This alignment promoted a more extensive hydrogen bond network and acted as a physical barrier against enzyme attack. These findings are in line with the FTIR and digestion analysis. Changes in the morphological micro-structure of granular were further determined (Fig.3.4). Chili pepper powder showed stacked layers (Fig.3.4b), while wasabi appeared conical with crumbly flakes (Fig.3.4c). In contrast to the polygonal irregular shape of CT (Fig.3.4a), the granular of RRS (Fig3.4d) showed aggregated and smooth structure due to the lipid cross-linking effect and oil-enriched surface (Cervantes-Ramírez et al., 2020). A more aggregated cavity structure were exhibited in CRS (Fig3.4e) than RRS, which might due to the hydrogen bonds or van der Waals forces between starch and polyphenol and protein (X. Li et al., 2024). It is notable that WRS (Fig.3.4f) showed distinct internal structures characterized by a looser, porous gel matrix with irregularly thick walls compared to the other complexes. This looser structure leads to easier enzyme access (Liu et al., 2023), which was consistent with our starch hydrolysis results. Similar irregular pore-like gel matrix morphology was observed in rice starch-protein (casein, whey protein isolate, and soy protein isolate) and polyphenols (ferulic acid, gallic acid, and quercetin) complexes, while the size of the grids varied depending on the type and of supplement polyphenol used (Wang et al., 2021). The morphology of rice starch-polyphenols (ferulic acid (FA), gallic acid (GA), and quercetin (QC)) were also reported by Han et al. (2020) reported on the morphology of rice starch-polyphenol complexes (ferulic acid, gallic acid, and quercetin), noting that all samples displayed a

pore-like gel matrix with thick walls. However, the size of the grids varied depending on the type of polyphenol used. It suggested that nutritional compounds (e.g., polyphenol and protein type) probably dominated granular structure behavior in the mixture.

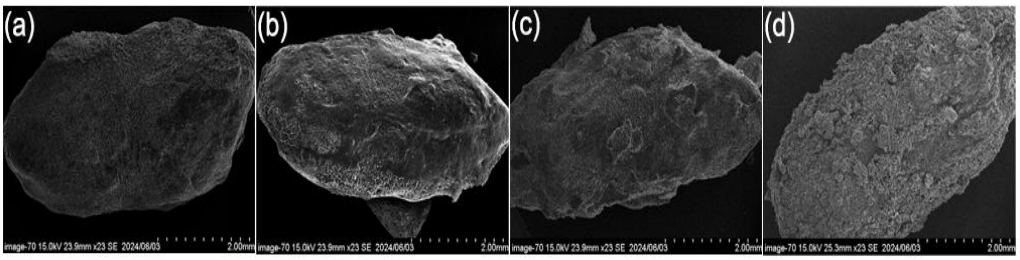

Fig. 3.3. Morphological attributes of Intact rice grains adding with different supplements. Notes: (a) normal cooked rice (CT); (b) cooked rice adding rapeseed oil (RRS); (c) cooked rice adding dried chili pepper powder (CRS); (d) cooked rice adding dried wasabi powder (WRS), scale bars show 2 mm.

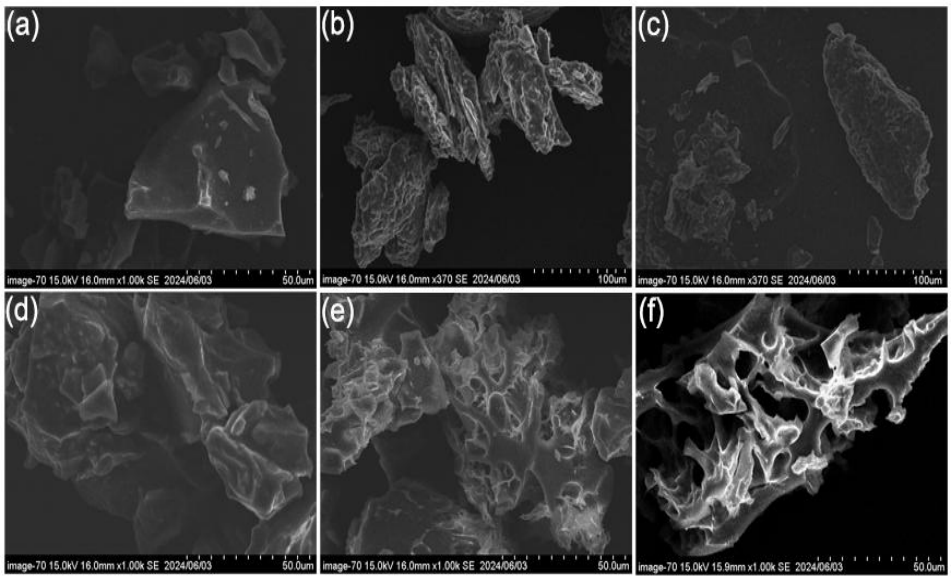

Fig. 3.4. Morphological attributes of rice starch granules and supplements. Notes: (a) normal cooked rice (CT); (b) dried chili pepper powder; (c) dried wasabi powder; (d) cooked rice adding rapeseed oil (RRS); (e) cooked rice adding dried chili pepper powder (CRS); (f) cooked rice adding dried wasabi powder (WRS), scale bars show 50 μm.

3.3.4. Principal component analysis

To further explore a correlation among various supplements and

physicochemical properties of cooked rice, PCA was established to obtain linear combinations of texture properties, moisture content, crude protein content and *in vitro* digestibility properties. As shown in the loading plot (Fig.3.5.), the total data variance (with PC1 contributing 53.32% and PC2 contributing 36.86%) of 90.18% was elucidated. The projection of the CRS and WRS samples were clustered together in quadrants 4 while the CT and RRS samples were clustered in quadrants 1 and 3, respectively, indicating a clear difference among the samples based on various supplements. The samples added with supplements revealed the highest values of RS, SF and OF, while negatively correlated with eGI and C_∞, indicating that supplements might promote compact molecular structure, thus contributing to prevent enzyme approaches and interaction. Furthermore, the CRS and WRS had the highest values of CP content and OF, indicating that protein might play a more important role in constructing the order structure in these samples. These results confirmed the previous analysis.

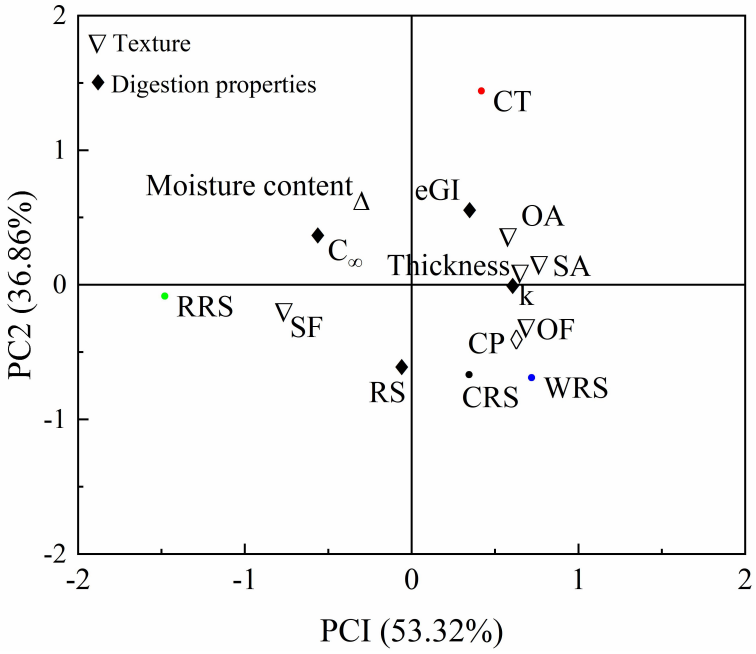

Fig. 3.5. Loading plot of Principal component analysis (PCA) for the first two principal components of cooked rice samples with varied supplements. Notes: CT: normal cooked rice (control); RRS: cooked rice adding rapeseed oil; CRS: cooked rice adding dried chili pepper powder; WRS: cooked rice adding dried wasabi powder. SF: surface firmness. OF: overall firmness. SA: surface adhesiveness. OA: overall adhesiveness. CP: crude protein content. RS: resistant starch content. eGI: estimated glycemic index.

3.4. Conclusions

Molecular level investigations and starch hydrolysis kinetic parameters showed that the presence of supplements contributed to the clumping and crosslinking of starch, thus affecting structure and digestive characteristics. The addition of supplements increased the levels of resistant starch (RS) in all samples. FT-IR and SEM results revealed that interactions were primarily driven by noncovalent bonds, where the guest chemistry component could influence rice starch to form short-range ordered structure in crystalline regions (eg. V-amylose, starch-protein/polyphenols complexes). These results were consistent with principal component analysis (PCA) analysis. This study extends a better understanding of starch-supplements interactions and their effects on the multi-scale structures, which could facilitate the applications of varied supplements to develop novel starchy functional foods. Since this study has mainly focused on the effect of supplement types on the attributes of cooked rice, further work should test whether the concentration of supplements and their composition are related to the low digestibility.

CHAPTER 4

Effects of adding various supplements on physicochemical properties and starch digestibility of cooked rice

4.1 Introduction

Rice, along with wheat and corn, is one of the major cereals all over the world. It primarily consists of starch which has been widely regarded as energy source for human nutrition (Lehmann and Robin, 2007). However, due to its high proportion of rapidly digested starch (RDS), white rice is classified as a high glycemic index (GI) food with a GI index of 83.40 ± 15.93, which may increase the risk of metabolic syndromes, such as obesity and cardiovascular disease (Kaur et al., 2016; Atkinson et al., 2021). Currently, numerous strategies are being explored for converting RDS into slowly digested starch (SDS) and resistant starch (RS) through physical and chemical modifications. Incorporating foods or nutrients aligning with dietary habits has attracted increasing attention because of its high security and consumer acceptability. For example, Krishnan et al. (2020) demonstrated decreased glucose release by adding extracted phenolics from pigmented rice to white rice.

Adding individual fatty acids (FAs), which bind into the helix structures of the amylose/amylopectin molecular chain through hydrophobic effect to form V-type RS, is also considered an effective strategy to decrease starch digestibility (Kawai et al., 2012; Zabar et al., 2009). Several studies have revealed that the ability of the V-type inclusion complex to retard the enzyme susceptivity is significantly affected by several factors, such as aliphatic chain properties, unsaturation degree, and composition of the fatty acid (FA) (Wang et al., 2016). Many researchers have also focused on applying pure starch, protein, and individual FAs to reveal the mechanism of changes in rice starch digestibility; however, the intact grains and edible oil have not yet been thoroughly studied. The interactions between digestion characteristics and lipid-modified starch were also consistently ignored and may not be well observed.

Lipids, as aggregates of triacylglycerols and micronutrients, were widely applied for household and industrial processing of starch-based food, including pre-frying

(risotto in Italy; paella in Spain), immersion (pilaf in Asia), and frying (fried rice in Asia) (Paesani and Gómez, 2021). Existing research on the formation of different lipid starch complexes varies due to differences in lipids and FAs. RO and MO were chosen as different fatty acid chromatogram where long-chain unsaturated fatty acids (UFAs) were dominant in RO and short-chain saturated fatty acids (SFAs) were dominant in MO (Ye and Lu, 2022; McKenzie et al., 2021). Okumus et al. (2018) found the enhanced conversion fractions of RS after adding hydrogenated sunflower oil and palmitic acid to cooked starch (10%, w/w), an opposite result that no complexes were formed between corn starch and corn oil was also reported by (Chen et al., 2017); however, the analysis on the effects of lipids composition and distribution lacked. Additionally, multiple nutritional compounds contained in lipids might also inhibit the activities of digestive enzymes (Chi et al., 2019), while these nutrients were rarely measured. Meanwhile, the presence of oil during the cooking process was reported to influence heat-mass transfer, thereby affecting the structure and physicochemical properties of starch and starchy food products (Krishnan et al., 2020), which could mean that temperature changes during treatment processes must be considered as a crucial factor. Yet, detailed monitoring of the temperature is sometimes lacking. Based on the previous research, the digestibility of oil-modified starch was generally related to the inhibited enzyme activity and physical barrier effects from granular or molecular structure, which are mainly influenced by dense gel structure processes and presence of other food ingredients (Paesani and Gómez, 2021). Furthermore, we hypothesized that the shell architecture of modified rice granular during mass transfer and heat transfer processes in an oil-water system could slow down the entry of enzymes. At the same time, the distributed lipids could also prevent enzyme approaches and interaction.

This study aims to analyze the mechanism related to how lipid addition manipulations affect the culinary and nutritional qualities of rice. For this purpose, the FA composition and nutritional value of lipids, such as rice bran oil (RO) and medium chain triglyceride oil (MO), were studied in detail as the basis for the experiment. Subsequently, the regulatory mechanism of starch digestion through the interaction between lipids and intact grains was inferred from the structure, digestive system environment, and mass-heat transfer characteristics.

4.2 Materials and methods

4.2.1. Materials and chemical reagents

White rice variety (*Oryza sativa* L. cv. Koshihikari, harvested in October 2022, Chiba, Japan), rice bran oil (RO) and MCT oil (MO) were purchased from local supermarkets (Matsudo, Chiba, Japan). The glucose oxidase/peroxidase kit (GOPOD) was purchased from Megazyme International Ireland Ltd. (Wicklow, Ireland). Pepsin (porcine gastric mucosal, ≥ 250 units/mg solid), pancreatin from porcine pancreas (hog pancreas, activity 8 × USP), invertase from baker's yeast (grade VII, ≥ 300/mg solid), trifluoroacetic acid, and the methyl esters of fatty acid were purchased from Sigma-Aldrich Co., Ltd. (St. Louis, MO, USA). All other reagents were of analytical grade and purchased from Sigma-Aldrich Chemical Co. (Shanghai, China).

4.2.2. Sample preparation

The lipid-rice complexes were prepared as described by Krishnan et al. (2020) and Kumar et al. (2018) with slight modifications. Rice grains (50 g) were cooked at a ratio of 1:1.5 (rice:deionized water, w/w) for 25 min as non-lipid-modified counterparts. Similarly, 10% (lipid:rice, w/w) of the dry weight basis of RO and MO were evenly dripped into the rice with a pipette at a constant speed under two different addition manipulations: before and after cooking, respectively, to obtain the starch-lipid complexes. The samples were obtained by adding RO before cooking (RB), adding MO before cooking (MB), adding RO after cooking (RA), and adding MO after cooking (MA). In before cooking mode, the lipid was uniformly added into raw rice grains before the addition of water. Meanwhile, in after cooking mode, lipid was added after cooking the rice. Afterwards, cooked grains were transferred into petri dishes wrapped in cling film then placed in an incubator (A0601-2V, Ikuta, Japan) at 35 °C for 25 min to equilibrate moisture. Then, a portion of the cooked grains was collected for further determination of moisture, texture, and *in vitro* digestibility. Other portions of cooked grains were freeze-dried and passed through a 200 sieves mesh. The obtained rice flour was sealed and stored in an aluminum bag at 4 °C for further analysis. The historical temperature evolution curve of the temperature of rice was measured using a fluorescent fiber optic thermometer (FL-2000, Anritsu, Tokyo, Japan).

4.2.3. Moisture content

Approximately 5.0 ± 0.2 g each of cooked grains and complexes were weighed and dried at 105 °C for 48 h in an air oven (Oven 8150, Labserv, Longford, Ireland), and the moisture content (% w.b.) was calculated according to the standard method of the Association of Official Analytical Chemists (AOAC, 2004) as the percentage weight loss difference in weight before and after drying by the formula：

$$\text{Moisture content}\ (\%) = (W_b - W_a)/W_b \times 100$$

where, W_b and W_a are the weight of powder before and after drying in oven, respectively.

4.2.4. Fatty acid (FA) profile and nutritional quality determination

Prior to analyzing the composition of fatty acids using GC-MS (QP2010 Shimadzu, Japan) with a flame ionization detector (FID), the fatty acid methyl esterification (FAME) was prepared as described by H. Wang et al. (2019) with minor modifications. Then, fatty acid methyl esters were then injected into a capillary (DB-5MS 30 m × 0.25 mm × 0.25 μm) with injector and detector temperature of 240 °C. High-purity helium was used as the carrier gas with a linear velocity of 1.0 mL/min. The oven temperature was programed to 60 °C for 5 min, raised to 150 °C at a heating rate of 15 °C/min; held for 2 min, then to 195 °C at a rate of 3 °C/min maintained 1 min, and finally to 220 °C at 1 °C/min rate and maintained for 1 min. A volume of 1.0 μL was injected at a split flow of 10 mL/ min and the split ratio was 1/10. The mass spectra were operated by electronic impact (EI) mode at 70 eV using the scan mode (m/z 50-450). The FA composition was identified by comparing the chromatogram retention time with the standards and expressed by area normalization as a relative percentage according to the following equation:

$$FA_i\ (\%) = \frac{A_{si} \times K_{FAMEi-FAi}}{\sum A_{ti} \times K_{FAMEi-FAi}}$$

where FA_i is the percentage of a certain FA composition; A_{si} and A_{ti} are the peak areas of each FAME in the sample for single and total; $K_{FAMEi\text{-}FAi}$ is the conversion coefficient of FAME to FA.

The nutritional quality was further determined by quantifying the atherogenic (AI)

and thrombogenic (TI) indices based on the results of FA according to Ulbricht and Southgate (1991) using the following equations:

$$\mathrm{AI} = \frac{\mathrm{FA}_{\text{Lauric acid}} + 4 \times \mathrm{FA}_{\text{Myristic acid}} + \mathrm{FA}_{\text{Palmitic acid}}}{\sum MUFA + \sum n-3\ PUFA + \sum n-6\ PUFA}$$

$$\mathrm{TI} = \frac{\mathrm{FA}_{\text{Myristic acid}} + \mathrm{FA}_{\text{Palmitic acid}} + \mathrm{FA}_{\text{Stearic acid}}}{0.5 \times \sum MUFA + 0.5 \times \sum n-6\ PUFA + 3 \times \sum n-3\ PUFA + (\frac{\sum n-3 PUFA}{\sum n-6 PUFA})}$$

where AI is the atherogenic index; TI is the thrombogenic index; MUFA is monounsaturated FA and PUFA is polyunsaturated FA.

4.2.5. Analysis of phytochemical components

Total phenolic content (TPC) of lipid samples was determined according to the procedure mentioned by Suri et al. (2020) with some modifications. Briefly, each 0.1 mL lipid solution (1.0 mg/mL n-hexane) taken in the amber glass test tube was sampled into 3 mL Na_2CO_3 (0.02 mg/mL) and 0.75 mL of Folin-Ciocalteu reagent (10-fold diluted). The resulting solution was homogenized and incubated at ambient temperature for 60 min before reading the absorbance at 710 nm. All experiments were conducted in triplicate with data expressed as mg gallic acid equivalent (GAE) per 1g of lipid.

4.2.6. Color measurements

Cooked rice grain samples were placed on a black panel to measure the CIELAB color coordinates using a colorimeter (CM-700d, Konica Minolta, Tokyo, Japan). Color readings were randomly performed at room temperature on twenty different locations of the sample. The average value was recorded as L*, a* and b* where L* represents lightness to darkness, a* represents redness to greenness and b* represents yellowness to blueness. Chroma (C*) was determined using the following equation:

$$\mathrm{C}^* = \sqrt{(\mathrm{a}^*)^2 + (\mathrm{b}^*)^2}$$

4.2.7. Texture analysis

The creep meter (RE2-3305S, Yamaden Co. Ltd., Tokyo, Japan) equipped with 10 Kg load cell was used to determine the firmness and adhesiveness of cooked rice samples. A single cooked grain was placed on a cylindrical baseplate and compressed twice using a planar plunger (Ø56 mm) at 1 mm/s once the surface temperature

reached 30 °C. Two positive and negative curves of the texture profile were obtained. The surface firmness and overall firmness in the positive region were referred to the force at 25% and 90% compression ratio of the original height with the contact point set as 0.005 N and 0.02 N trigger force, respectively. Meanwhile, surface and overall adhesiveness were defined as the corresponding negative region of the texture profile and sample thickness corresponded to the distance between the plunger and baseplate (Tamura et al., 2022a). Approximately 20 cooked grains were determined within 15 min to avoid changes in moisture and textural properties.

4.2.8. Determination of the complexing index (CI) of the starch-lipid complexes

The CI of the starch-lipid complexes was characterized following the approach described by Wang et al. (2019). In brief, 0.4 g of each rice powder collected from Section 2.2 was dispersed with ultrapure water to achieve a total weight of 5.0 g in a 50 mL centrifuge tube and heated in boiling water for 15 min with occasional shaking (every 3 min). Then, the gelatinized mixture was treated further with 5 times dilution, vortexed and centrifuged at 3000g for 15 min after cooling to ambient temperature. The supernatant of 0.5 mL prepared in the previous step was further diluted 30 times and stained by 2 mL iodine solution for 10 min. The maximum absorbance was recorded at 620 nm using a UV-2600 spectrophotometer (Shimadzu Co., Japan) and the CI was calculated using the following formula:

$$\mathrm{CI} = (\mathrm{A_S} - \mathrm{A_{S-l}})/\mathrm{A_S} \times 100$$

where A_S and $A_{S\text{-}l}$ are the absorbance of the original starch solution and starch-lipid complex solution, respectively.

4.2.9. Fourier transform infrared (FTIR) spectroscopy

The FTIR spectra of freeze-dried starch powder were recorded using a Fourier transform spectrophotometer (DJK Corporation, Japan) equipped with a DLaTGS detector and KBr beamsplitter. The spectra were scanned using an Attenuated Total Reflection (ATR) sampling technique in the range of 4000–400 cm^{-1}. 64 of accumulation scans at a resolution of 2 cm^{-1} were collected (Krishnan et al., 2020b).

4.2.10. Dynamic analysis of in vitro enzymatic hydrolysis

About 170 g of 4% total starch (TS) equivalent cooked grains were subjected to a two-stage simulated gastro-intestinal *in vitro* digestion model (Tamura et al., 2022b). Simulated gastric fluid (SGF) and intestinal fluid (SIF) were performed to mimic starch hydrolysis. The experiment condition has been reported by previous study (Tamura et al., 2016). The digestive solution (0.5 mL) was collected and mixed thoroughly with 95% ethanol (3 mL) to analyze the glucose content after 5, 15 and 30 min of gastric digestion and after 5, 10, 15, 20, 30, 60, 90, 120, 180, 240, 300, 360 and 480 min of intestinal digestion. The mixed supernatants were then centrifuged at 1800×g for 15 min and incubated at 37 °C for 15 min with amyloglucosidase and invertase. The glucose concentration of the incubated samples was determined using the D-glucose assay kit (GOPOD, Megazyme International Ireland Ltd, Ireland). Percentage of starch hydrolysis ($\%S_H$) was calculated using the following equation:

$$\%S_H = S_h/S_i = 0.9 \times G_p/S_i$$

where S_h,S_i and G_p are the mass of hydrolyzed starch, initial total starch and glucose produced, respectively. A conversion factor (0.9) calculated fromthe molecular weight of starch monomer/ glucose (162/180 = 0.9) (Goñi et al., 1997), was used. A first-order equation model established by Goñi et al. (1997) was performed to determine the kinetics of starch hydrolysis.

$$C = C_\infty\left(1 - \exp^{-kt}\right)$$

where C and C_∞ represent the hydrolysis percentage and equilibrium percentage, respectively; k corresponds to the kinetic constant and t corresponds to the digestion time.

Determination coefficient (R^2) was used to evaluate the fitting quality of the first-order equation model.

$$R^2 = 1 - \frac{\sum_{i=1}^{N}(C_{exp,\,i} - C_{pre,\,i})^2}{\sum_{i=1}^{N}(C_{exp,\,i} - C_{ave})^2}$$

where, $C_{exp,\,i}$ and $C_{pre,\,i}$ represent the percentage of hydrolyzed starch and predicted hydrolyzed starch of the ith experiment, respectively. C_{ave} corresponds to the average experimental $\%S_H$. N corresponds to the number of observations.

The hydrolysis index (HI) was defined as the area of the hydrolysis curve of cooked grain samples divided by white bread (Choujuku; Pasco Shikishima, Aichi, Japan).

The eGI was calculated using the formula from Goñi et al. (1997):

$$\mathrm{eGI} = 39.71 + 0.549\mathrm{HI}$$

4.2.11. Morphology and tissue structure

The surface of the cooked grains was measured using a digital camera (DS-5M; Nikon, Tokyo, Japan) and all image process parameters in terms of focus, lighting and shutter speed, were standardized for each individual component. Scanning electron microscopy (SEM) (SU1510; Hitachi High-Tech, Tokyo, Japan) was also used to examine the micro-structure changes of the external and internal conditions of grains. The freeze-dried samples were mounted and examined under a SEM at 5 kV in high vacuum mode. The obtained images were processed by graphic software (Photoshop, Adobe, San Jose, CA, USA).

4.2.12. Statistical analysis

All results were described as the mean ± standard deviation and analyzed by one-way analysis of variance (ANOVA) in conjunction with Tukey's test to assess the significance of differences ($p < 0.05$) using SPSS 21.0 software (IBM, Chicago, USA). Analyses were performed at least in triplicate for each sample. Comparisons between cooking conditions were performed with T-test. The figures and PCA analysis were processed using Origin 2018 (Origin Lab, California, USA).

4.3 Results and discussion

4.3.1. Moisture content

The moisture content (MC%) of cooked rice is presented in Table 4.1. Significant difference in the cooking conditions and type of lipids were observed ($p < 0.05$). The MC% of complexes decreased significantly (54.04%-51.06%) after modification using oil compared to CT with value of 55.50% ($p < 0.05$), which was similar to previous study (Tamura et al., 2022a). It is noticeable that the lipid added with before mode (51.06%-51.91%) exhibited the maximum decrease compared to the after mode (53.88%-54.04%). These results might be attributed to the higher heat and mass transfer rate under before heating conditions (Su et al., 2018). As described in Fig. 4.1., rice cooked with lipids exhibited faster heating curve due to the lower

specific heat capacity of lipids, especially RO (1.8-2.4), compared to water (4.2) (Tochitani and Fujimoto, 2001), leading to an accelerated mass transfer rate and evaporation of water. Similar observations have been reported in potato strips fried with different lipid types. The highest temperature evolution curve and corresponding minimum moisture content were observed in sample fried with lard compared to other lipid types (Li et al., 2020). Moreover, higher heating temperature conditions can break hydrogen bonds, thus decreasing the number of hydroxyl groups which can result in lower water absorptivity of starch granules (Romano et al., 2018, Li et al., 2020). Nevertheless, no significant differences were observed between before mode and after mode, suggesting that the loss of moisture content was mainly attributed to the heating process.

Table 4.1. The moisture content, chromatic parameters, and complexing index of cooked rice samples with various lipid adding conditions.

Sample	Moisture content (% w.b.)	L*	a*	b*	C*	CI
CT	55.50±0.85 a	68.30±1.11 a	-1.78±0.06 a	4.83±0.37 bc	5.15±0.36 bc	-
RO_BC	51.06±1.31 c	64.36±2.06 c	-2.19±0.16 d	5.58±0.49 a	5.60±0.49 a	18.50±0.22 b
RO_AC	53.88±0.72 b	66.29±1.16 b	-2.01±0.10 c	4.93±0.33 bc	5.33±0.33 b	28.31±0.87 a
MO_BC	51.91±0.14 c	65.43±1.04 bc	-2.04±0.09 c	4.98±0.53 b	5.39±0.47 b	14.28±0.44 c
MO_AC	54.04±0.18 b	65.90±1.53 b	-1.90±0.08 b	4.55±0.11 c	4.94±0.31 c	27.87±0.32 a

CT: normal cooked rice (control). RO: cooked rice with rice bran oil; MO: cooked rice with medium chain triglyceride (MCT) oil; BC: before cooking; AC: after cooking. CI: complexing index. Different lower-case letters in the same column indicate significant differences ($p < 0.05$). Each value in the table is expressed as mean ± standard deviation. The sample number (n): moisture (n = 4-5); chromatic parameters (n = 10-12); CI (n = 4-5).

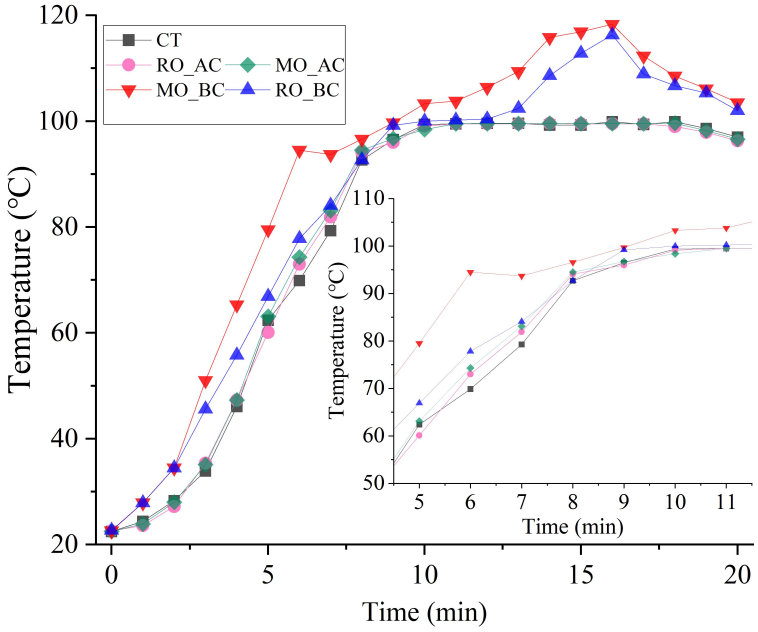

Fig. 4.1. The historical temperature evolution curve of the temperature of rice cooked with different lipids and addition manipulation. *Notes:* The historical temperature evolution curve from 5 min to 11 min were further shown in insert figure. CT: normal cooked rice (control). RO: cooked rice with rice bran oil; MO: cooked rice with medium chain triglyceride (MCT) oil; BC: before cooking; AC: after cooking.

4.3.2. Fatty acid (FA) composition

Fatty acid (FA) composition is not only a critical quality index of lipids, but also a vital factor on the starch-lipid complexes. As described in Table 4.2. and pie chart Fig.4.2., 9 kinds of fatty acids were detected in RO, and the dominant UFAs such as oleic acid (C18:1, n-9) and linoleic acid (C18:2, n-6) accounted for 41.54% and 32.38%, respectively. Meanwhile, palmitic acid (22.53%) was the major saturated fatty acids (SFAs) in RO. Similar results have been reported by Ramezanzadeh et al., (2000) in which 75.6% to 81.7% of UFAs were found in rice brand oil. FA composition could vary significantly due to variety, extraction methods, processing technique and storage conditions (Ye and Lu, 2022). Therefore, this underlines the fact that molecular proportions of FAs are more important than the types of lipids. Among 8 kinds of fatty acid in MO, SFAs, such as octanoic acid and octanoic acid, covered a dominating amount equivalent to 65.23% and 33.29%, respectively. Presence of other minor UFAs such as palmitoleic acid, oleic acid and linoleic acid was also detected, which might be due to the nature of extracted and refined raw materials which is coconut (Wickramasinghe Mudiyanselage and Wickramasinghe,

2023). FA chromatogram clearly indicated that long-chain UFAs were dominant in RO, whereas short-chain SFAs were dominant in MO. Generally, UFAs in diets have the potential to reduce plasma LDL cholesterol levels and cardiovascular disease risks (Shuai et al., 2022). Lipid-modified starch, which can form a V-shaped crystalline structure, are known as type 5 resistant starch. It has several physiological benefits such as production of short-chain fatty acids (SCFAs) and regulation the gut microbes (Li et al., 2022). The stability of complexes towards enzyme digestibility has been related to chain length and saturation of fatty acid (Kang et al., 2021). In relation to this, susceptibility of potato starch to α-amylolysis has been clarified to decrease with the increase of linoleic acid content (Kapusniak and Siemion, 2007). Kang et al. (2021) found out that steamed bread starch supplemented with lauric acid showed a higher RS content and dense structure which is less digestible by enzymes compared to sample with stearic acid. Another study reported that the addition of RO at a ratio of 2.5% resulted in the highest SDS and RS contents (Luangsakul and Ritudomphol, 2018a). Furthermore, lower AI and TI were associated with decreased atherogenic fatty acids and therefore lowers the risk of cardiovascular disease (Xiang et al., 2023). The values of AI and TI were calculated to be between 0.33 to 1.21 and 0.57 to 1.11 in RO and MO, respectively (Table 4.2). These were 2-8 times lower than the values reported for commercial palm lipids (AI: 2.7; TI: 3.5) (Mancini et al., 2015), suggesting that these two kinds of lipids have the potential for improving resistance to digestion and decrease the risk of cardiovascular disease as a result of lipid modification.

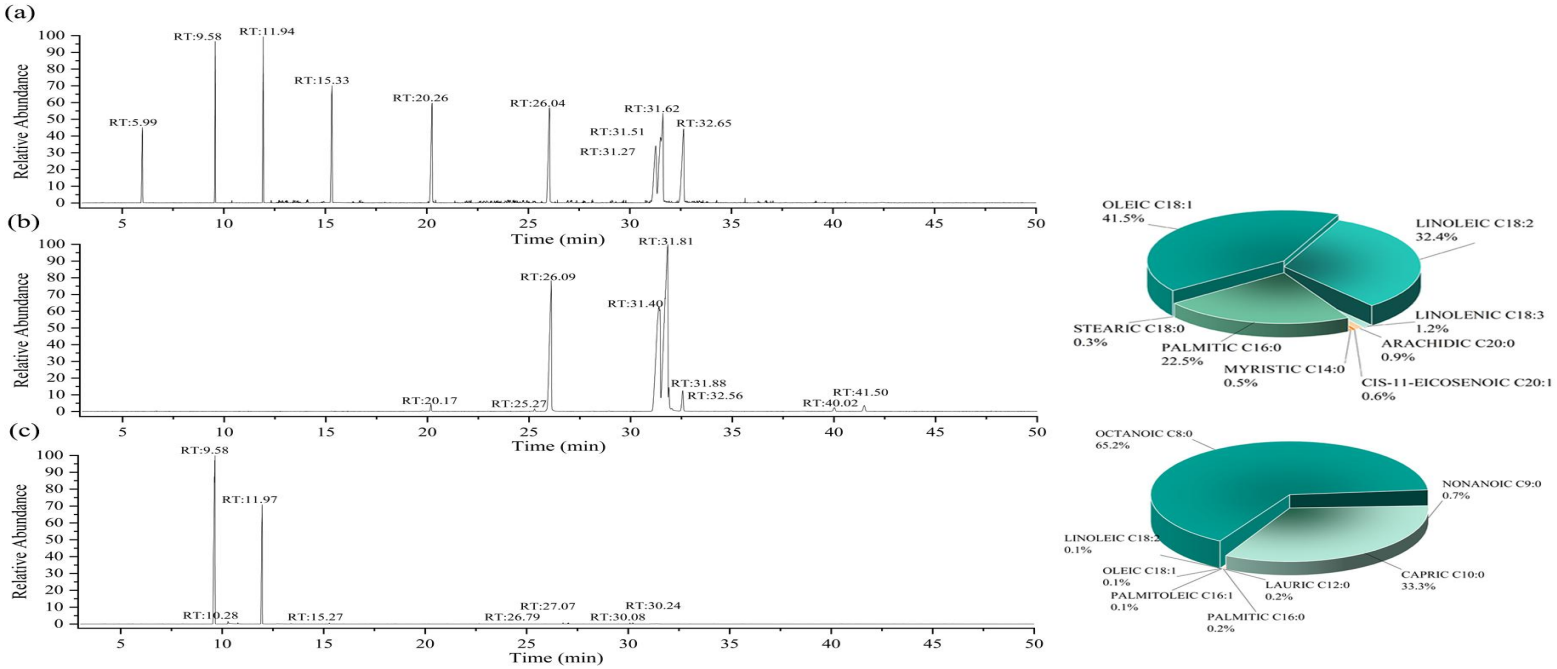

Fig. 4. 2. Gas Chromatography-Mass Spectrometry chromatograms of the fatty acid methyl esters present in the lipid types. *Notes:* (a) fatty acid methyl esters standard, (b) rice bran oil (RO), (c) MCT oil (MO). Fatty acid methyl esters were prepared from the lipids and the proportion of saturated and unsaturated fatty acids were identified based on standard retention time (RT). 3D-Pie chart depicts the fatty acid profile. [RT-5.99: hexanoic acid ME, RT-9.58: octanoic acid ME; RT-10.28: nonanoic acid ME; RT-11.94: decanoic acid ME; RT-15.33:lauric acid ME, RT-20.26: myristic acid ME, RT-25.27: palmitoleic acid ME, RT-26.04: palmitic acid ME, RT-31.27 : linoleic acid ME, RT-31.51: linolenic acid ME, RT- 31.62: oleic acid ME, RT-32.65: stearic acid ME, RT-40.02: cis-11-Eicosenoic acid ME, RT-41.50: arachidic acid ME.]

Table 4. 2. The fatty acids compounds and nutrient composition analysis of lipid.

Component[b]	ID[a]	Lipid number	Rice bran oil[c]	Medium chain triglyceride oil[c]
Octanoic acid	A, B, C	C8:0	ND	65.23±0.27
Nonanoic acid	B, C	C9:0	ND	0.73±0.01
Decanoic acid	A, B, C	C10:0	ND	33.29±0.11
Lauric acid	A, B, C	C12:0	ND	0.22±0.01
Myristic acid	A, B, C	C14:0	0.54±0.04	ND
Palmitic acid	A, B, C	C16:0	22.53±0.13	0.19±0.04
Palmitoleic acid	B, C	C16:1n-7	0.04±0.01	0.14±0.02
Stearic acid	A, B, C	C18:0	0.25±0.07	ND
Oleic acid	A, B, C	C18:1n-9	41.54±0.28	0.11±0.01
Linoleic acid	A, B, C	C18:2n-6	32.38±0.19	0.09±0.03
Linolenic acid	A, B,C	C18:3n-3	1.24±0.10	ND
Arachidic acid	B, C	C20:0	0.93±0.05	ND
cis-11-Eicosenoic acid	B, C	C20:1n-9	0.55±0.03	ND
Saturate fatty acid		ΣSFA	24.25±0.29	99.66±0.44
		ΣMUFA	42.13±0.32	0.25±0.03
		ΣPUFA	33.62±0.29	0.09±0.03
Unsaturate fatty acid		ΣUFA	75.75±0.61	0.34±0.06
ΣSFA/ΣUFA			0.32±0.01	299.24±42.72
Σn-6 PUFA/Σn-3 PUFA			26.11±0.05	ND
AI			0.33±0.01	1.21±0.06
TI			0.57±0.01	1.11±0.03
Total phenolic content (mg GAE/g)			0.83±0.09	0.14±0.03

[a]ID: The identification was indicated by the following symbols, A = mass spectrum and retention time (RT) agree with the authentic standard compound that run under the same GC-MS conditions, B = mass spectrum and retention time agree with literature data: (1) (Xiang et al., 2017), (2) (Krishnan et al., 2020b), (3) (Ye and Lu, 2022). C = tentative identification based on interpretation of mass spectrum and comparison with similar compounds.
[b]Component: compounds of fatty acid with positive and negative matching >800.
[c]Relative content: the mean values of parallel experiment. ND: not detected.

4.3.3. The chromatic parameters of cooked rice

The chromatic parameters are shown in Table 4.1. Surface color of cooked grains was significantly altered by the type of lipid and cooking process ($p < 0.05$).

Compared to CT, the complexes showed a lower L* value while a*, b* and C* values were higher, except for MA. CT had the highest observed L* value which could be illustrated by the fact that more free water on the grain surface favors light reflection (Santos et al., 2018). Similar observation was explained by Heredia et al. (2014) wherein L* values of French fries were positively correlated with the moisture. Meanwhile, the increased chromatic parameters of a* and b* during deep-lipid frying were due to the formation of Maillard reaction products (MRPs). The carbonyl groups (reducing sugar, aldehyde, ketone) have been reported to interact with amino groups (free amino acids, peptide, protein) in rice and lipids via covalent bonding in the presence of heat, leading to browning (Wang et al., 2023). These findings are consistent with our experimental results of RB and MB samples. Additionally, the initial high pigmentation in RO, which caused color intensification even without prolonged heating, contributed to higher a* value in RA (Thanonkaew et al., 2012).

4.3.4. Texture analysis

The firmness, thickness and adhesiveness parameters are shown in Fig. 4.3. Partial gelatinization of starch granules could occur under high heat and humid conditions due to swelling of starch molecules (Lin et al., 2023). Concurrently, swelling of rice kernels lead to formation of more cracks which contributed to easier leaching of amylose and small amylopectin molecules chains (Liu et al., 2023). These starch materials attach to the rice surface and affect firmness and adhesiveness through cross-linked bonds with proteins, polyphenol etc. (Paesani and Gómez, 2021). As shown in Fig.4.3a, CT has the lowest surface firmness (SF) and thickness peak. After lipid modification, RA and MA showed an increased SF and a forward-shifted thickness peak, probably because cross-linked bonds between lipid molecules and leached starchy materials reinforced the starch granule structure, as well as limited water absorption and granule swelling (X. Li et al., 2022). Compared with after mode, RB and MB had higher SF, which might be related to the higher heating temperature evolution curve of lipid-water phase as shown in Fig. 2 which can lead to dissolution of more amylose molecules (Pu et al., 2013). Subsequently, the presence of lipids can induce more polymerization of starch granules into large clusters because of hydrophobic properties and adhesion effect, enabling the cross-linked network structure to be firmer (Yang et al., 2016). Moreover, penetration of high-temperature

lipids into pores and cavities emptied after evaporation of water contributed to cell structural integrity and form harder crust, preventing granules from swelling (Ding et al., 2018). This phenomenon was also supported by the lower thickness of RB and MB. It is worth noting that the double peak of thickness and dispersion of texture parameters in the before mode is probably due to lipid deposition and uneven heat exposure. Ngadi et al. (2007) demonstrated that the hardness of crust is related to fatty acid profile of different lipids. Their results showed that the hardness increased with increasing SFA and degree of hydrogenation, whereas reverse trend was observed with increasing UFA and trans isomers fatty acids content. In contrast with their observation, Wang et al. (2020) reported that the UFA comprising cis-double bonds disrupted the arrangement of FA in the single-helix cavity of amylose cavity, which might also pose hydrophobic environment for quaternary and ternary non-covalent bonded complexes (e.g., starch with proteins, lipids and polymeric phenols, etc.). The RB exhibited the higher SF compared to MB with a high UFA content, potentially due to the higher TPC, thus, resulting in a more compact complexes (Wang et al., 2023). Similar observations have also been found out by Li et al. (2020) who investigated the fries fried with 10 kinds of lipid. Their results revealed that fries fried in lard lipid exhibited the highest puncture force (0.71 N) followed by palm lipid (0.68 N) and rice bran lipid (0.64 N) which is consistent with this study. Contrary to SF, overall firmness (OF) of lipid-modified samples decreased both in before and after mode. This is due to variation in the mixture triglycerides. Generally, larger molecular size lipid, compared to single fatty acid, tends to form an obvious lipid-enriched phase on the starch granule surface which prevented moisture reduction and kept moisture inside the granules leading to a moist core (Wang et al., 2019). Previous study observed a clear water-lipid boundary (more moisture in the core than at edge) of fried fries by proton density images using MRI. Results also revealed that there is a corresponding increase in texture curve at hard lipid-filled crispy crust and sudden decrease at soft interior core (Li et al., 2020), which was similar with our results. However, the OF of those discrete values were higher than CT, indicating incubation process could not affect excessively dehydrated granule structure. For adhesiveness, the CT exhibited highest surface (SA) and overall adhesiveness (OA) compared to other samples. A significant decrease in adhesion of pre-fried rice was reported by Paesani and Gómez (2021), whereas no correlation has been reported between adhesiveness and the measurements of damaged starch or meal rate. This

finding suggested that the SA and OA might be related to the adherence of lipids on the outer layers of the grain and poor dispersity of hydrophobic lipid during heating process, rather than the changes in the starch (Tamura et al., 2022a).

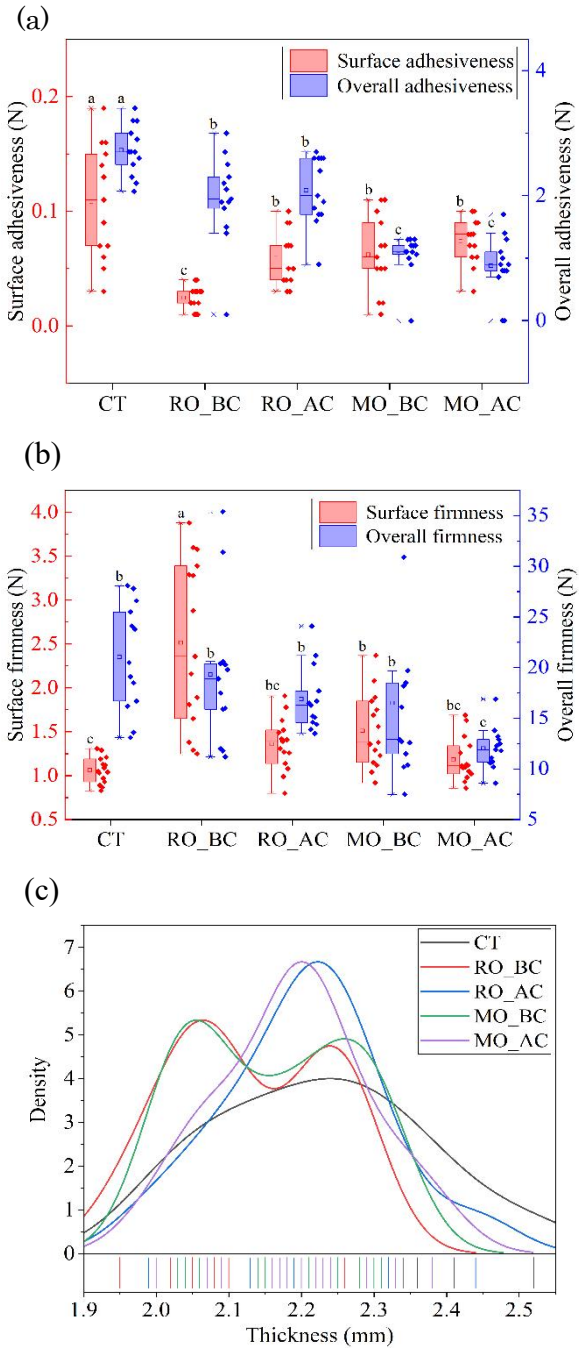

Fig. 4.3. The texture parameters of the rice grains cooked with different lipids and addition manipulation. Notes: (a) surface and overall firmness, (b) surface and overall adhesiveness, (c) thickness. The sample number (n): firmness (n = 12-15); adhesiveness (n = 12-15); thickness (n = 12-15). Significant differences generated from two-way ANOVA ($p < 0.05$) are also represented. The * letter shows the differences between same parameters.

4.3.5. Binding ability of starch-lipid complexes

The complexing index (CI) represents the degree of starch-lipid complexes formation. As described in Table 4.1., the CI ranged from 14.28% to 28.31%. The CI could be influenced by fatty acid (composition, chain length, unsaturation degree, etc.), bioactive substance and treatment process (Krishnan et al., 2020b). The cooking conditions had a significant impact on CI as before mode (ranged from 14.28% to 18.50%) is significantly lower than after mode (ranged from 27.87% to 28.31%) ($p < 0.05$), which might be related to the degree of starch gelatinization (Luangsakul and Ritudomphol, 2018a). At pre-phases of before condition, binding efficiency was limited due to high integrity of the starch granules. Also, incomplete gelatinization of starch affected the diffusion of the starch molecular chain and hindered further binding with FAs (Tamura et al., 2021). Due to the higher temperature of the water-lipid phase, gelatinization proceeds and lead higher moisture content at this stage. Meanwhile, water migrated from inside to outside the molecules hindering lipids from entering the starch paste (Chang et al., 2014). Wang et al. (2019) studied the effect of moisture content on CI and found out that excessive water content (> 40%) prevented the binding of starch–lipid complexes in both glutinous rice (GRS) and high-amylose corn starch (HACS). Furthermore, a portion of the starch granules lose their cavity structure and form a lamellar structure with a smooth surface during high temperature, which also prevents the absorption of fatty acids (Kuang et al., 2017). These observations were consistent with our SEM micrograph results. In addition, significant differences in CI were observed between fatty acid types. Notably, among the heating conditions, the maximum CI was observed in RA which is rich in long-chain UFA. Wang et al. (2016) concluded that the CI decreased with increasing carbon chain length of FAs. Similar observations were reported by Kawai et al., (2012) wherein SCFAs formed more complexes and higher CI due to better accessibility and interaction with helical cavity of gelatinized starch. However, these studies were limited to single fatty acid only and did not include the effects of lipid application or additional manipulation. The contrary results observed might be due to the matrix composition. The major matrix components (total starch, amylose, amylopectin, proteins, lipids and phenolics) have been known to play a role in complex formation (Quek and Henry, 2015). Previous study clarified that proanthocyanidins molecules might combine with amylose through H-bonding to

form type II intra-helical inclusion complexes (Amoako and Awika, 2019). Li et al. (2020) also pointed out that phenolics might form complexes and be stabilized by non-covalent CH-π bonds along α-(1 → 4) glycosidic chains. It was assumed that SCFAs of MO were easier to form complexes than RO while the higher content of phenolics squalene, pigments, oryzanol, etc. in RO contributed to the reversed trend and a higher CI. Similar results were reported by Krishnan et al., (2020a) wherein rice bran oil rich in UFA exhibited highest CI with white rice compared to coconut lipid (CO) and virgin coconut lipid (VCO) regardless of before, during and after conditions even though CO and VCO contained more SCFAs. However, higher CI indicated the formation of starch-lipid complexes, which might be related to higher proportion of RS but not to lower glycaemic response. Krishnan et al. (2020) also demonstrated that red rice cooked with RO had the lowest glycaemic response while the highest CI was observed in black rice samples. These findings indicated that dense molecular configuration of complexes resisting enzymatic digestion was more important than the quantity of complexes formed.

4.3.6. FTIR analyses of the starch-lipid complexes

FT-IR spectra of the cooked rice, complexes as well as lipids are presented in Fig. 4.4. The FTIR spectrum showed characteristic starch samples IR patterns with transmittance peaks around 990 cm^{-1} due to the C−O of C−O−C glycosidic linkages in the polysaccharide and a broad band in the range 3100-3500 cm^{-1} attributed to the stretching vibrations of primary and secondary alcoholic groups. In contrast to CT, two additional absorption bands at 2856 and 1748 cm^{-1} were observed in all complexes, which were attributed to asymmetric and symmetric stretching vibrations of $-CH_3$ and $-CH_2$ in the fatty acids and vibration of carbonyl (Krishnan et al., 2020). Furthermore, the reduced peak intensity around 3400 cm^{-1} suggesting the reduction of hydroxyl groups, correspond to a reduced hydrogen bond interaction among starch molecules (Mathew & Abraham, 2007). Similar spectrum was observed by Wang et al. (2019) where the most obvious peak was found with the highest complexing degree. In addition, complexes revealed absorption bands around 1616, 1539 and 1447 cm^{-1}, attributed to the stretching of aromatic rings. It is noteworthy that new signals appeared around 1683 and 1435 cm^{-1}, which confirmed a possible interaction between starch and polyphenols. The bands of complexes located at 1615, 1558, 1520, 1455,

1373 cm^{-1} also had shifted and diminished while band at 815 cm^{-1} disappeared. Similar shifted and diminished bands were observed in GA (gallic acid)-RS and QC (quercetin)-RS complexes owing to the interaction between gallic acid, quercetin and rice starch (Han et al. 2020). Rice cooked at MB mode showed lower intensity in the 1447 to 1685 cm^{-1} region, which might be due to the reduced phenolic content during deep-lipid frying (Krishnan et al., 2020). This suggested that an interaction between rice starch and polyphenols might also contributing to the shifting and disappearance of absorption peaks of complexes.

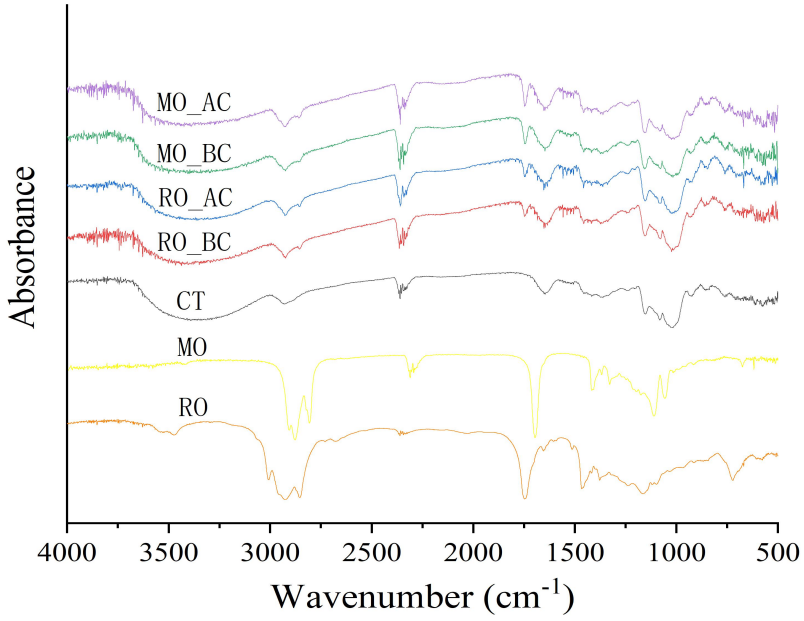

Fig. 4.4. Fourier transform infrared spectroscopy spectra of cooked rice grains with different lipids and addition manipulation. *Notes:* CT: normal cooked rice (control). RO: cooked rice with rice bran oil; MO: cooked rice with medium chain triglyceride (MCT) oil; BC: before cooking; AC: after cooking.

4.3.7. In vitro digestion and kinetics analysis

The starch hydrolysis of cooked rice grains with and without lipid addition during gastro-small intestinal *in vitro* digestion is summarized in Fig. 4.5. During simulated gastric digestion, nearly no starch hydrolysis was observed. This might be related to the action of pepsin in SGF which mainly digests proteins, however, it was considered since the physical properties could be altered by the digestive environment of the stomach (Tamura et al., 2016a). Moreover, the particle diameter of lipid

emulsions was also influenced by gastric juice (Krishnan et al., 2020b). Increased droplet sizes of lipid particles were observed due to flocculation between whey protein and lipid, which occurs under acidic condition during gastric digestion period (Liu et al., 2021). In addition, other factors such as pH value of stomach, mechanical shear from gastric peristalsis could also alter the coagulation degree of lipid emulsions (Singh and Sarkar, 2011). A stable droplet size in the later stages of gastric digestion was also reported by Guo et al. (2017). It was due to the increased elasticity of the lipid which contributed to coverage on the rice surface. Starch hydrolysis percentage (SH%) was significantly affected by addition manipulation and type of lipid in a downward trend and almost reached equilibrium at I420 (from 80.92% to 91.31%) compared with CT (95.85%) wherein RB showed the lowest SH%. Similar observations on adding time have been reported by Krishnan et al. (2020) in which lowest glycaemic response was observed in the RO group with before and during compared with after condition. This could be contributed to easier fitting of hydrocarbon tail of lipids within the helical cavity of amylose, known as type V RS, during gelatinization rather than completed gelatinization (Zabar et al., 2009). Moreover, among the lipid types studied, the maximum glycemic potency was observed in MO. This might be due to self-assembling of the endogenous protein or phenolics present in RO to form a compact ordered structure through non-covalent interactions, which becomes type I RS protecting the entrapped starch fraction. Such structure and substances are very few in MO (Li et al., 2020; Wang et al., 2020).

To compare the percentage of starch hydrolysis numerically, the experimental data were fitted to a first-order equation model (Goñi et al., 1997). As summarized in Table 4.3., the kinetic parameters were significantly affected by lipid types and addition manipulation. In general, RB (88.07) had a lower C_∞ than the others (92.66-105.55) especially compared with CT ($p < 0.05$). The k was in the range between 0.47 and 0.86 min^{-1}, with some significant differences. However, it is noteworthy that the addition of all lipids with before mode presented a higher k contrary to lower C_∞ values, which might be related to lower enzyme resistance in the early stage of small intestinal digestion especially MO (I5-I180). It is presumed that a portion of leached starch of before mode was more susceptible to destruction due to higher temperature. Simultaneously, surface starch particles encapsulated in lipids were easily exposed to intestine enzymes due to natural surfactants of bile salts (Na^+, K^+, and $PO4^+$) promoting the digestive degradation of lipids (Xiang et al., 2023). High

R^2 of all samples was considered to accurately depict starch digestibility. Hydrolysis index (HI) and estimated glycemic index (eGI) were significantly reduced whereas no statistically difference was observed between MB and CT. Source of origin of fatty acid type as well as polyphenol concentration have also been considered vital in forming stable complexes resistant to amylolysis (Amoako and Awika, 2019). Long chain fatty acid-starch complexes are known to form more stable V-type crystalline configuration compared to short and medium chain, wherein ideal packing into amylose helix has been assumed (Wang et al., 2020). Conversely, UFA was found to impair the formation of compact structures and affect the crystallinity (Zabar et al., 2009). On the other hand, Luangsakul and Ritudomphol, (2018b) observed that rice with rice bran oil, which was the richest source of UFA (linoleic acid, C18:2), had the highest relative crystallinity in XRD patterns and lowest eGI. In this research, the same result was observed even when the cooking condition and the rice variety were altered. This could be due to the presence of polyphenols entangled with amylose/long branch chains of amylopectin or sandwiched between amylose through H bonds to form polyphenol-starch complexes (Chi et al., 2018). The lower polyphenol content in MO and oxidation loss of before mode were consistent with these finding. Additionally, the inhibition of polyphenols against enzymes might also play a key role in starch digestion (Zhang et al., 2020; Pan et al., 2019). Therefore, we further speculated that the differences among kinetic parameters were due to the combination of inhibition effects and the physical barriers formed by fatty acids, bioactive substances and lipid film itself which prevent or suppress the enzymes-starch bindings.

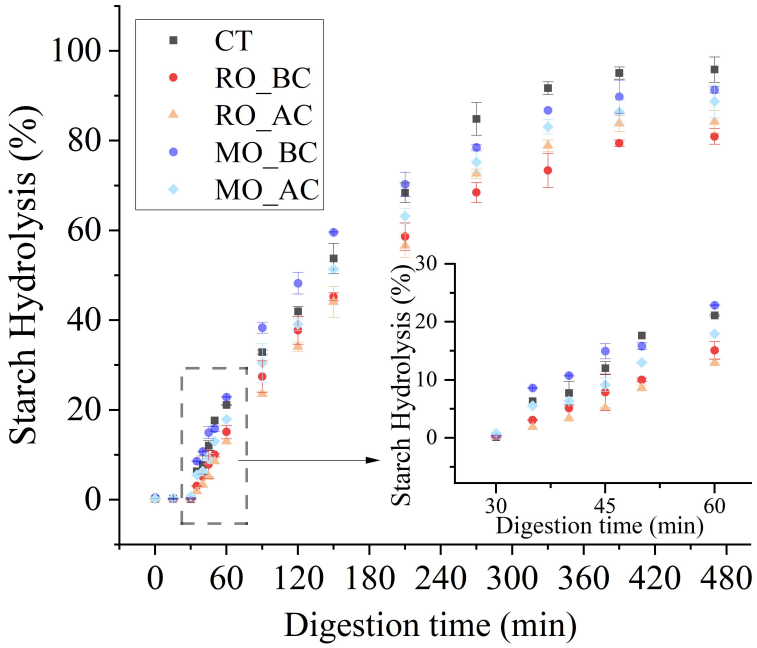

Fig. 4.5. Changes in starch hydrolysis (%) of cooked rice grains with different lipids and addition manipulation. *Notes:* Error bars represent standard deviation (n = 3-6). CT: normal cooked rice (control). RO: cooked rice with rice bran oil; MO: cooked rice with medium chain triglyceride (MCT) oil; BC: before cooking; AC: after cooking. The changes in starch hydrolysis (%) of cooked rice grains from 30 min to 60 min were further shown in insert figure.

Table 4.3. The kinetic parameters of starch hydrolysis of cooked rice samples with various lipid adding conditions.

Sample	C∞ (%)	$k \times 10^{-2}$ (min^{-1})	R^2	HI	eGI
CT	105.6±3.4 a	0.62±0.05 b	0.99	77.2±1.3 a	82.1±0.7 a
RO_BC	88.1±0.6 c	0.61±0.01 b	0.98	64.0±0.2 c	74.8±0.1 c
RO_AC	101.6±3.4 a	0.47±0.03 c	0.95	64.6±1.3 c	75.2±0.7 c
MO_BC	92.7±1.9 b	0.86±0.05 a	0.99	77.5±0.7 a	82.2±0.4 a
MO_AC	96.5±1.7 ab	0.62±0.03 b	0.97	70.6±0.6 b	78.5±0.4 b

CT: normal cooked rice (control). RO: cooked rice with rice bran oil; MO: cooked rice with medium chain triglyceride (MCT) oil; BC: before cooking; AC: after cooking. Mean ± standard deviation. The sample number (n): C_∞ (n = 3-6); k (n = 3-6); HI (n = 3-6); eGI (n = 3-6). Different letters within the same column indicate significant differences ($p < 0.05$).

4.3.8. Morphology analysis

Changes in the morphological and microstructure characteristics of cooked rice grains are shown in Fig. 4.6. Compared to grains cooked with water, the complexes shown more evident morphological differences especially the before mode, in which the Maillard reaction and layered structure were more pronounced due to deep frying

and uneven distribution of oil. SEM images of CT displayed characteristic shapes of cooked rice in relatively smooth sphere with pore-like structures, many cracks and voids in the tissue structure and cells (Tamura et al., 2022b). Different from non-oil-modified samples, the modified complexes were observed to have an obvious oil-enriched surface phase and transparent granular structure, with formation of large clusters and protrusion caused by the agglomeration and lipid cross-linking effect of gelatinized starch granules. The physical barriers would quantitatively coat the starch tightly, which prevented the interaction between the starch and enzymes and reduced the starch hydrolysis rate. However, the lipid layer adhered unevenly on the surface through weak crosslinking which could be easier to lose due to shear force of gastric and pancreatic juices (Zhao et al., 2023). These results were partly consistent with the kinetic data.

Additionally, it was seen that granular structures collapsed and melt because of the cooking process. Such damage in the natural crystalline structure was expected for starch sources (Okumus et al., 2018). In contrast to native starch with coarse porous structure inside, totally different structure was detected after lipid modification. The voids generated by water evaporation and mass/heat transfer were filled by lipids resulting in smooth section among complexes especially in after mode (Fig. 4.6.c, g, k, o, s). Moreover, in contrast to the polygonal cell wall structure of CT due to separation of hydrated and swollen starch granules, RB and MB exhibited completely different internal structures (Fig. 4.6.g, h, o, p). A portion of starch granules lost the intact structure due to high temperature, which demonstrated that the rice starch suffered rapid gelatinization distortion and compaction into a whole mass that led to creation of a hollow structure inside the rice grains (Li et al., 2020). On the other hand, another portion of starch maintained their granular and intact starch granules with an angular and surface, suggesting that cross-linking bonds formed by lipids could enhance the starch granule structure and form V-type resistant starch, increasing the tolerance of starch to high temperature and enzyme attack (Zhao et al., 2022a). These findings are in line with the CI and digestion analysis. It suggested that the structure of lipid-starch complexes might have significant effects on the physicochemical properties, such as pasting, gelatinization, enzyme susceptibility, crystallinity and solubility (Zhao et al., 2023). Similar results were reported in which a complete destruction was detected in brown lentil starch added with stearic acid and olive oil, while a moderately protected granular structure were evident after corn oil and soy oil

were added (Okumus et al., 2018). It is worth noting that samples with added RO contained particles with more regular and angular surface than MO, which might be attributed to the bioactive substances (Li et al., 2020). These results and SEM micrographs insinuated that the trends observed in molecular research even span throughout the micro-structural level. Therefore, it can be inferred that the intact granule forms, strengthened dense structure and lipid layer are important factors affecting its digestion characteristics.

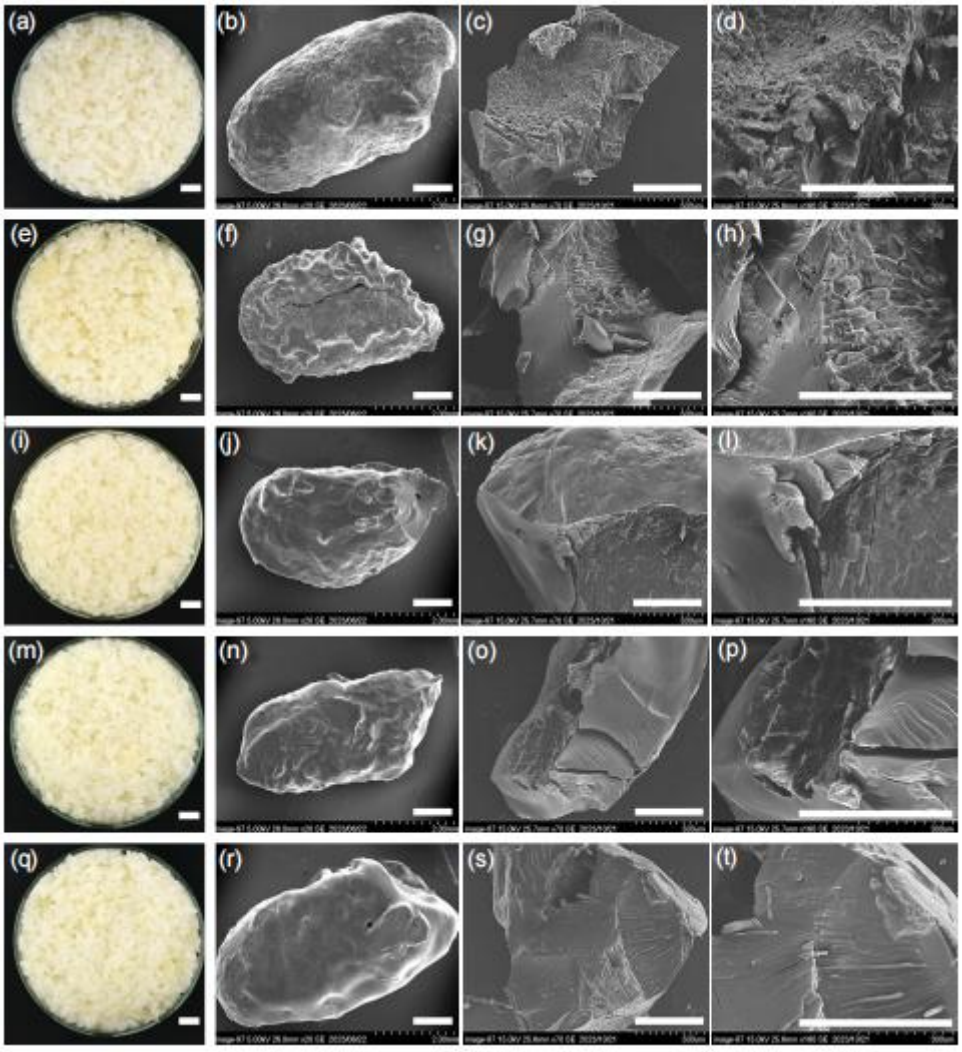

Fig. 4.6. Morphological attributes of cooked rice with different lipids and addition manipulation. *Notes:* (a-d) normal cooked rice (CT); (e-h) rice cooked with RO at before condition; (i-l) rice cooked with RO at after condition; (m-p) rice cooked with MO at before condition. (q-t) rice cooked with MO at after condition. a, e, i, m and q show appearance of cooked rice samples, scale bars show 10 mm; b, f, j, n and r show surface of intact rice grain, scale bars show 1 mm; c, g, k, o and s show internal status of samples, scale bars show 500 μm. d, h, l, p and t show further detailed internal status of samples, scale bars show 500 μm.

4.3.9. Principal component analysis

To establish a correlation between the treatment method and quality properties of cooked rice, PCA was performed to obtain linear combinations of temperature, color, texture properties, lipid composition, and in vitro digestibility. As shown in Table 4.4., PCA analysis revealed that the first two principal components (PCs) elucidate 81.49% of the total data variance (PC1 contributing 56.11% and PC2 contributing 25.38%). The loading plot (Fig. 4.7.) visualizes the differentiation among the samples. The projection of the RO group onto the space of the two first PCs was clustered together in quadrant 2 and the MO group in quadrants 3 and 4. In contrast, the CT group was in quadrant 1, indicating a clear difference among the samples based on lipid types. The samples subjected to RO_BC and MO_BC had the highest values of temperature and complexing index, indicating that the heat and mass transfer of the cooking process played a more important role in texture properties. Furthermore, TPC, UFA, and SFA subjected to RO_BC and MO_BC were positively correlated with the SF and CI. On the contrary, TPC, CI, and SF were negatively correlated with starch hydrolysis properties, which suggests that the nutrition compounds and distributed lipids might promote compact molecular structure and physical barrier effects, thus contributing to preventing enzyme approaches and interaction. These results confirmed the previous analyses.

Table 4.4. The correlation of variables to factors in Principal Component Analysis (PCA) of cooked rice samples with varied lipid addition manipulations.

Variables	PC1 (56.11%)	PC2 (25.38%)
Temperature	-0.201	-0.199
Moisture content	0.255	0.189
L*	0.256	0.194
a*	0.286	0.070
b*	-0.245	0.080
C*	-0.241	0.059
SFA	0.013	-0.401
MUFA	-0.232	0.247
PUFA	-0.232	0.248
UFA	-0.232	0.247
TPC	-0.246	0.201
Starch hydrolysis	0.269	0.032
Surface firmness	-0.269	-0.012
Overall firmness	-0.021	0.254
Surface adhesiveness	0.287	0.060
Overall adhesiveness	0.035	0.384
Thickness	0.246	0.207
Complexing index	-0.129	-0.057
eGI	0.216	-0.186
C∞	0.231	0.245

SFA: saturated fatty acids. MUFA: monounsaturated fatty acids. PUFA: polyunsaturated fatty acids. UFA: unsaturated fatty acids. TPC: total phenolic content. L*: lightness to darkness. a*: redness to greenness. b*: yellowness to blueness. eGI: estimated glycemic index.

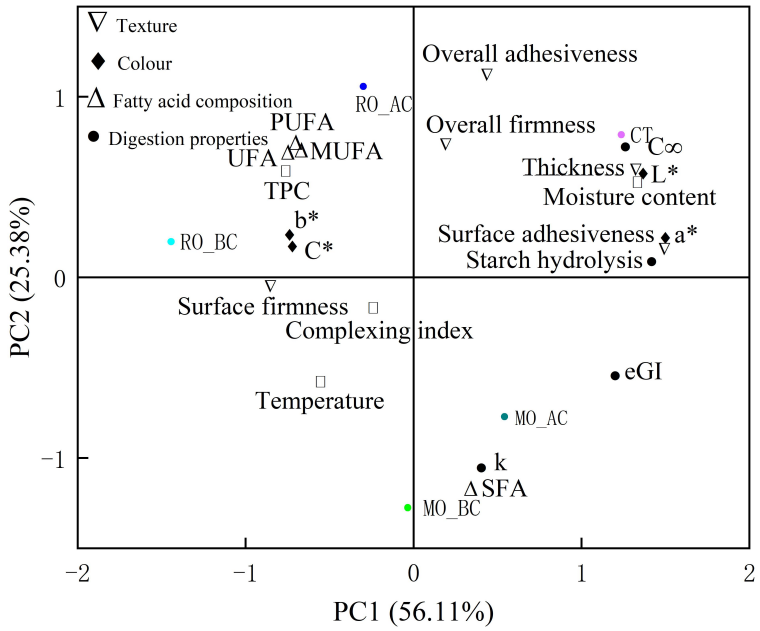

Fig. 4.7. Loading plot of Principal component analysis (PCA) for the first two principal components of cooked rice samples with varied addition manipulations. *Notes:* SFA: saturated fatty acids. MUFA: monounsaturated fatty acids. PUFA: polyunsaturated fatty acids. UFA: unsaturated fatty acids. TPC: total phenolic content. L*: lightness to darkness. a*: redness to greenness. b*: yellowness to blueness. eGI: eGI: estimated glycemic index.

4.4. Conclusions

Microstructure characteristics and kinetic parameters depicted hereby showed that the presence of lipid barriers and lipid addition manipulation contributed to clumping and cross-linking of gelatinized starch particles to maintain its complete shape as demonstrated in the results wherein RB exhibited significantly decreased starch hydrolysis and eGI. Bioactive ingredient content, CI as well as FTIR spectrum demonstrated that the guest chemistry component affected some of the dense structural attributes of V-amylose. The PCA results suggested lipid types and addition manipulation were essential in cooked rice structure and digestibility. In general, these results highlighted the potential of lipids as a phytochemical resource that can be used to develop possible low glucose release starch-based functional food. Further work should test and evaluate if multiscale micro-structure differences can be observed and whether there are other critical contributors related to the low digestibility.

CHAPTER 5

Conclusions and future plan

5.1. Conclusion

Starch is the main component of many foods and the main source of energy in human diet (Shuai et al., 2022). Natural starch exists in the form of insoluble semi-crystalline particles and has a very complex multi-layered structure system (Li et al., 2020). After natural starch granules are heated in water, they will undergo a series of processes including water absorption, swelling, double helix unwinding and microcrystalline melting (irreversibly destroying the internal molecular order), polysaccharide leaching, and swelling of the granules. Amylose will leach out from inside the granules (Tamura et al., 2022; Chang et al., 2014; Kuang et al., 2017). When there is a suitable ligand in the system, amylose can be induced to form a loose helical conformation. This creates a helical structure with a hydrophobic cavity that provides a high-affinity binding site for ligands (Kang et al., 2021; Luangsakul and Ritudomphol, 2018; Wang et al., 2023). When other additives such as lipids and polyphenols are present in the system, they will combine to form complexes, thereby changing many structural and functional properties of starch, thereby affecting the taste and taste of starch-based foods. Flavor, digestibility, etc. Polyphenols are considered functional ingredients beneficial to human health due to their special properties (such as antioxidant, anti-tumor, enzyme inhibition, etc.) (Han et al. 2020; Zhang et al., 2020; Pan et al., 2019). Many researchers have reported that polyphenols are able to reduce the rate of starch hydrolysis by inhibiting the activity of digestive enzymes or acting as a physical barrier between enzymes and starch (Zhao et al., 2023). Starch and lipids can form starch-lipid complexes during processing (Li et al., 2020). Since the formation of starch-lipid complex will have a certain impact on the structure of starch, in vitro enzyme digestion and other properties, in recent years, there has been much research on starch (Okumus et al., 2018; Zabar et al., 2009). The

study of lipid-starch complexes has attracted widespread attention. The complex formed by amylose and lipid is also classified as a new type of resistant starch (RS), namely RS5 (Amoako and Awika, 2019). After RS enters the large intestine, it can be fermented by intestinal flora to produce short-chain fatty acids (SCFAs) (Quek and Henry, 2015). SCFAs play an important physiological role in maintaining intestinal health and human health (Quek and Henry, 2015; Amoako and Awika, 2019).

This study investigated the physicochemical modifications of cooked rice caused by adding various supplements (rapeseed oil, dried chili pepper, and wasabi powder). The cooked rice without adding anything had the lowest surface firmness (SF) compared to others, whereas the SF of rice grains increased with the presence of additives (Table 2.1.). Compared with CRS (0.80 ± 0.14 N) and WRS (0.77 ± 0.03 N), the SF of RRS increased significantly to 0.95 ± 0.08 N, which can be explained mainly by water evaporation during the equilibrium period. Water migration from inside to outside was further promoted by the low moisture content of the dried chili pepper powder and dried wasabi, resulting in a quick moisture loss on the surface of the rice grains, which might contribute to a higher SF. However, the change in overall firmness (OF) showed the opposite trend to the surface firmness. Harder cores of rice grains were observed in CRS (18.14 ± 1.53 N) and WRS (17.88 ± 0.91 N), which might be related to continuous water migration from the inside to the outside due to a moisture content difference between dried chili pepper powder and dried wasabi powder. In contrast, RRS (15.02 ± 1.11 N) showed a significantly softer core than CT (16.43 ± 2.08 N). This could be related to the triglycerides in oil. The RRS showed the lowest SA ($1.43 \pm 0.25 \times 10^{-2}$ N), which could be explained by the formation of the lipid-enriched phase. Overall adhesiveness (OA) was found to be not significantly different with the lowest OA showing in RRS (2.33 ± 0.29 N) as well. The changes in OA and SA were considered due to the physical barrier of the supplements. The cooked rice grain with dried wasabi and red chili pepper powder showed lower moisture content (48.22 ± 1.18% w.b. and 48.49 ± 1.00% w.b.) than the control (54.90 ± 0.85% w.b.). The decrease in MC% might be attributed to the lower MC% of dried wasabi and red chili pepper powder

(Table 2.2.). In contrast, rice grains added with oil showed the least reduction of MC% (52.63 ± 1.06% w.b.), which was likely due to the surface lipid layers affecting the evaporation of water. The CP content of CRS and WRS was significantly increased by the addition of dried chili pepper powder and dried wasabi powder (Table 2.2.). The reason might be that proteins are one of the main biomolecules found in seed material. All rice samples exhibited a decreased digestion pattern compared with CT during the simulated small intestine digestion process (Fig. 2.1.), which might be related to the interaction between starch and various guest molecules. All samples showed significantly lower eGI compared with CT (Table 2.3.), suggesting that the addition of lipids and phenols in carbohydrate-rich foods might be a practical means to reduce the glycemic response of starchy food eaten worldly. Compared to the control group, two absorption peaks at 2856 and 1748 cm^{-1} and new signals at 1683 and 1435 cm^{-1} appeared in the Fourier transform infrared (FTIR) spectroscopy (Fig. 3.2.). Analysis of FTIR results revealed that the interaction force was mainly through noncovalent interactions. Moreover, adding supplements increased the resistant starch (RS) levels in all samples (Fig. 3.1.). Scanning electron microscope (SEM) suggested that oil-enriched phase, proteins, and polyphenols could cause large agglomeration and loose gel structure (Fig. 3.3., Fig. 3.4.). The cracks on the grain surface facilitate the leaching of amylose and small amylopectin molecules, which might interact with polyphenols, proteins, and other nutritional ingredients by hydrogen bonds, hydrophobic interactions, or other molecular forces, subsequently attaching on the grain surface to form a gel network, changing the firmness and adhesiveness as well as digestibility and hydrolysis kinetic parameters of the starch (Wang et al., 2023). Lipid coating on starch surface also contributed to physical barriers between digestive enzymes and starch, which together with the emulsification speed in intestinal environment, could affect the digestion process (Wang et al., 2023; Shuai et al., 2022). At the same time, gelatinization net architecture of granule during *in vitro* gastro-small intestinal digestion system might prevent enzyme action, wherein the distributed nutrition compounds might also slow down the access of enzyme (Pan et al., 2019).

The fatty acid composition of lipids was always ignored in starch digestibility field although it was considered as an essential research foundation in lipid-starch complexes. Thus, the influence of lipid modification and thermal treatment on the physicochemical properties and starch digestibility of cooked rice prepared with varied addition manipulations was further investigated. the lipid added with before mode (51.06%-51.91%) exhibited the maximum decrease compared to the after mode (53.88%-54.04%). These results might be attributed to the higher heat and mass transfer rate under before heating conditions (Su et al., 2018). Gas chromatography-mass spectrometry (GC-MS) was applied to establish the fatty acid profile (Fig. 4.2.). Moreover, the nutritional quality was further determined by quantifying the total phenolics, atherogenic (AI) and thrombogenic (TI) indices. FA chromatogram clearly indicated that long-chain UFAs were dominant in RO, whereas short-chain SFAs were dominant in MO. Different modification characteristics of starch were also observed between lipids and fatty acids. The values of AI and TI were calculated to be between 0.33 to 1.21 and 0.57 to 1.11 in RO and MO, respectively (Table 4.2.). These were 2-8 times lower than the values reported for commercial palm lipids (AI: 2.7; TI: 3.5) (Mancini et al., 2015), suggesting that these two kinds of lipids have the potential for improving resistance to digestion and decrease the risk of cardiovascular disease as a result of lipid modification. the increased chromatic parameters of a* and b* during deep-lipid frying were due to the formation of Maillard reaction products (MRPs) (Wang et al., 2023). CT has the lowest surface firmness (SF) and thickness peak (Fig. 4.3.). After lipid modification, RA and MA showed an increased SF and a forward-shifted thickness peak, probably because cross-linked bonds between lipid molecules and leached starchy materials reinforced the starch granule structure, as well as limited water absorption and granule swelling (X. Li et al., 2022). New signals appeared around 1683 and 1435 cm^{-1}, which confirmed a possible interaction between starch and polyphenols (Fig. 4.4.). Starch hydrolysis percentage (SH%) was significantly affected by addition manipulation and type of lipid in a downward trend and almost reached equilibrium at I420 (from 80.92% to 91.31%) compared with CT (95.85%) wherein RB showed the lowest SH%

(Fig. 4.5.). Moreover, among the lipid types studied, the maximum glycemic potency was observed in MO. This might be due to self-assembling of the endogenous protein or phenolics present in RO to form a compact ordered structure through non-covalent interactions, which becomes type I RS protecting the entrapped starch fraction (Chi et al., 2018). Such structure and substances are very few in MO (Li et al., 2020; Wang et al., 2020). Lipid coating on starch surface contributed to physical barriers between digestive enzymes and starch, which together with the type of lipids and the emulsification speed in intestinal environment, could affect the digestion process. At the same time, the heat and mass transfer during the cooking process influenced by the presence of oil-water phase, affecting the structure and physicochemical properties of starch. However, studies about these theories are very limited. Our results showed that shell architecture of granule during mass and heat transfer processes in oil-water system slowed down the access of enzyme, wherein the distributed lipids prevent enzyme action. It indicated that aside from treatment methods, temperature changes during the treatment process were also important factors (Yang et al., 2016). Based on these results, we hypothesized that the intact granule forms a strong and dense structure which significantly affect the digestion characteristics of lipid-starch complexes. These findings provide valuable insights about the digestibility mechanism of oil-modified starchy products and the applicability of lipid addition during rice cooking to enhance its nutritional functionality.

5.2. Future plan

Because this study focuses on the interactions between starch and various supplements by examining their short-range structures, morphological characteristics, physicochemical properties, and starch hydrolysis. Various techniques were used to characterize the mechanism and multi-scale structure of the obtained complexes, indicating that differences in the resistant starch content and digestion kinetic behaviors related to the in vitro digestion properties. Further structural research is necessary to better elucidate the impact of structure on starch digestion characteristics such as multi-scale structure including starch types (Type A, B, C, V). Meanwhile, as

food itself is a complex collection of compounds, the nutrients and antioxidants contained in the additives themselves are different. Therefore, the effects of different additive contents or single compounds isolated from the same additive on starch structure and digestion characteristics should be further considered.

References

Amoako, D.B., Awika, J.M., 2019. Resistant starch formation through intrahelical V-complexes between polymeric proanthocyanidins and amylose. Food Chem. 285, 326–333. https://doi.org/10.1016/j.foodchem.2019.01.173

Asemani, M., Rabbani, A.R., 2020. Detailed FTIR spectroscopy characterization of crude oil extracted asphaltenes: Curve resolve of overlapping bands. J. Pet. Sci. Eng. 185, 106618. https://doi.org/10.1016/j.petrol.2019.106618

Atkinson, F.S., Brand-Miller, J.C., Foster-Powell, K., Buyken, A.E., Goletzke, J., 2021. International tables of glycemic index and glycemic load values 2021: a systematic review. Am. J. Clin. Nutr. 114, 1625–1632. https://doi.org/10.1093/ajcn/nqab233

Bogusz, S., Libardi, S.H., Dias, F.F., Coutinho, J.P., Bochi, V.C., Rodrigues, D., Melo, A.M., Godoy, H.T., 2018. Brazilian *Capsicum* peppers: capsaicinoid content and antioxidant activity. J. Sci. Food Agric. 98, 217–224. https://doi.org/10.1002/jsfa.8459

Bordoloi, A., Singh, J., Kaur, L., 2012. In vitro digestibility of starch in cooked potatoes as affected by guar gum: Microstructural and rheological characteristics. Food Chem. 133, 1206–1213. https://doi.org/10.1016/j.foodchem.2012.01.063

Cervantes-Ramírez, J.E., Cabrera-Ramirez, A.H., Morales-Sánchez, E., Rodriguez-García, M.E., Reyes-Vega, M.D.L.L., Ramírez-Jiménez, A.K., Contreras-Jiménez, B.L., Gaytán-Martínez, M., 2020. Amylose-lipid complex formation from extruded maize starch mixed with fatty acids. Carbohydr. Polym. 246, 116555. https://doi.org/10.1016/j.carbpol.2020.116555

Chang, F., He, X., Fu, X., Huang, Q., Jane, J., 2014. Effects of Heat Treatment and Moisture Contents on Interactions Between Lauric Acid and Starch Granules. J. Agric. Food Chem. 62, 7862–7868. https://doi.org/10.1021/jf501606w

Chen, X., He, X.-W., Zhang, B., Fu, X., Jane, J., Huang, Q., 2017. Effects of adding corn oil and soy protein to corn starch on the physicochemical and digestive properties of the starch. Int. J. Biol. Macromol. 104, 481–486. https://doi.org/10.1016/j.ijbiomac.2017.06.024

Chi, C., Li, X., Feng, T., Zeng, X., Chen, L., Li, L., 2018. Improvement in Nutritional Attributes of Rice Starch with Dodecyl Gallate Complexation: A Molecular Dynamic Simulation and in Vitro Study. J. Agric. Food Chem. 66, 9282–9290. https://doi.org/10.1021/acs.jafc.8b02121

Chi, C., Li, X., Zhang, Y., Chen, L., Xie, F., Li, L., Bai, G., 2019. Modulating the in vitro digestibility and predicted glycemic index of rice starch gels by complexation with gallic acid. Food Hydrocoll. 89, 821–828. https://doi.org/10.1016/j.foodhyd.2018.11.016

Dartois, A., Singh, J., Kaur, L., Singh, H., 2010. Influence of Guar Gum on the In Vitro Starch Digestibility—Rheological and Microstructural Characteristics. Food Biophys. 5, 149–160. https://doi.org/10.1007/s11483-010-9155-2

Ding, Y., Yang, L., Xia, Y., Wu, Y., Zhou, Y., Wang, H., 2018. Effects of frying on starch structure and digestibility of glutinous rice cakes. J. Cereal Sci. 83, 196–203. https://doi.org/10.1016/j.jcs.2018.08.014

Farooq, A.M., Dhital, S., Li, C., Zhang, B., Huang, Q., 2018. Effects of palm oil on structural and in vitro digestion properties of cooked rice starches. Int. J. Biol. Macromol. 107, 1080–1085. https://doi.org/10.1016/j.ijbiomac.2017.09.089
Goñi, I., Garcia-Alonso, A., Saura-Calixto, F., 1997. A starch hydrolysis procedure to estimate glycemic index. Nutr. Res. 17, 427–437. https://doi.org/10.1016/S0271-5317(97)00010-9
Guo, Q., Bellissimo, N., Rousseau, D., 2017. The Physical State of Emulsified Edible Oil Modulates Its in Vitro Digestion. J. Agric. Food Chem. 65, 9120–9127. https://doi.org/10.1021/acs.jafc.7b03368
Han, X., Zhang, M., Zhang, R., Huang, L., Jia, X., Huang, F., Liu, L., 2020. Physicochemical interactions between rice starch and different polyphenols and structural characterization of their complexes. LWT 125, 109227. https://doi.org/10.1016/j.lwt.2020.109227
He, H., Zheng, B., Wang, H., Li, X., Chen, L., 2020. Insights into the multi-scale structure and in vitro digestibility changes of rice starch-oleic acid/linoleic acid complex induced by heat-moisture treatment. Food Res. Int. 137, 109612. https://doi.org/10.1016/j.foodres.2020.109612
Heredia, A., Castelló, M.L., Argüelles, A., Andrés, A., 2014. Evolution of mechanical and optical properties of French fries obtained by hot air-frying. LWT - Food Sci. Technol. 57, 755–760. https://doi.org/10.1016/j.lwt.2014.02.038
Herzallah, S., Holley, R., 2012. Determination of sinigrin, sinalbin, allyl- and benzyl isothiocyanates by RP-HPLC in mustard powder extracts. LWT 47, 293–299. https://doi.org/10.1016/j.lwt.2012.01.022
Igoumenidis, P.E., Zoumpoulakis, P., Karathanos, V.T., 2018. Physicochemical interactions between rice starch and caffeic acid during boiling. Food Res. Int. 109, 589–595. https://doi.org/10.1016/j.foodres.2018.04.062
Kang, X., Yu, B., Zhang, H., Sui, J., Guo, L., Abd El-Aty, A.M., Cui, B., 2021. The formation and in vitro enzymatic digestibility of starch-lipid complexes in steamed bread free from and supplemented with different fatty acids: Effect on textural and retrogradation properties during storage. Int. J. Biol. Macromol. 166, 1210–1219. https://doi.org/10.1016/j.ijbiomac.2020.11.003
Kapusniak, J., Siemion, P., 2007. Thermal reactions of starch with long-chain unsaturated fatty acids. Part 2. Linoleic acid. J. Food Eng. 78, 323–332. https://doi.org/10.1016/j.jfoodeng.2005.09.028
Kaur, B., Ranawana, V., Henry, J., 2016. The Glycemic Index of Rice and Rice Products: A Review, and Table of GI Values. Crit. Rev. Food Sci. Nutr. 56, 215–236. https://doi.org/10.1080/10408398.2012.717976
Kawai, K., Takato, S., Sasaki, T., Kajiwara, K., 2012. Complex formation, thermal properties, and in-vitro digestibility of gelatinized potato starch–fatty acid mixtures. Food Hydrocoll. 27, 228–234. https://doi.org/10.1016/j.foodhyd.2011.07.003
Krishnan, V., Awana, M., Samota, M.K., Warwate, S.I., Kulshreshtha, A., Ray, M., Bollinedi, H., Singh, A.K., Thandapilly, S.J., Praveen, S., Singh, A., 2020a. Pullulanase activity: A novel indicator of inherent resistant starch in rice (Oryza sativa. L). Int. J. Biol. Macromol. 152, 1213–1223.

https://doi.org/10.1016/j.ijbiomac.2019.10.218
Krishnan, V., Mondal, D., Bollinedi, H., Srivastava, S., Sv, R., Madhavan, L., Thomas, B., R, A.T., Singh, A., Singh, A.K., Praveen, S., 2020b. Cooking fat types alter the inherent glycaemic response of niche rice varieties through resistant starch (RS) formation. Int. J. Biol. Macromol. 162, 1668–1681. https://doi.org/10.1016/j.ijbiomac.2020.07.265
Kuang, Q., Xu, J., Liang, Y., Xie, F., Tian, F., Zhou, S., Liu, X., 2017. Lamellar structure change of waxy corn starch during gelatinization by time-resolved synchrotron SAXS. Food Hydrocoll. 62, 43–48. https://doi.org/10.1016/j.foodhyd.2016.07.024
Kumar, A., Sahoo, S., Sahu, S., Nayak, L., Ngangkham, U., Parameswaran, C., Bose, L.K., Samantaray, S., Kumar, G., Sharma, S.G., 2018. Rice with pulses or cooking oils can be used to elicit lower glycemic response. J. Food Compos. Anal. 71, 1–7. https://doi.org/10.1016/j.jfca.2018.05.003
Kumar, L., Brennan, M.A., Mason, S.L., Zheng, H., Brennan, C.S., 2017. Rheological, pasting and microstructural studies of dairy protein–starch interactions and their application in extrusion-based products: A review. Starch - Stärke 69, 1600273. https://doi.org/10.1002/star.201600273
Le Gall, S., Sole-Jamault, V., Nars-Chasseray, M., Le Goff, A., Le Bot, L., Guinet, T., Renaud, C., Gervais, J., Bansard, S., Ohleyer, L., Jeandroz, S., 2021. Data on agronomic traits, biochemical composition of lipids, proteins and polysaccharides and rheological measurement in a brown mustard seed collection. Data Brief 38, 107417. https://doi.org/10.1016/j.dib.2021.107417
Lehmann, U., Robin, F., 2007. Slowly digestible starch – its structure and health implications: a review. Trends Food Sci. Technol. 18, 346–355. https://doi.org/10.1016/j.tifs.2007.02.009
Li, M., Ndiaye, C., Corbin, S., Foegeding, E.A., Ferruzzi, M.G., 2020. Starch-phenolic complexes are built on physical CH-π interactions and can persist after hydrothermal treatments altering hydrodynamic radius and digestibility of model starch-based foods. Food Chem. 308, 125577. https://doi.org/10.1016/j.foodchem.2019.125577
Li, M., Wang, F., Wang, J., Wang, A., Yao, X., Strappe, P., Zhou, Z., Wu, Q., Guo, T., 2022. Starch acylation of different short-chain fatty acids and its corresponding influence on gut microbiome and diabetic indexes. Food Chem. 389, 133089. https://doi.org/10.1016/j.foodchem.2022.133089
Li, P., Wu, G., Yang, D., Zhang, H., Qi, X., Jin, Q., Wang, X., 2020. Analysis of quality and microstructure of freshly potato strips fried with different oils. LWT 133, 110038. https://doi.org/10.1016/j.lwt.2020.110038
Li, X., You, Y., Wu, L., Yang, J., Chen, H., Zheng, J., Zhang, F., 2024. Rheological properties, multiscale structure, and in vitro digestibility of a maize starch–konjac glucomannan–bamboo leaf flavonoid complex modified by dynamic high-pressure microfluidization. Food Chem. 139966. https://doi.org/10.1016/j.foodchem.2024.139966
Li, X., Yue, X., Huang, Q., Zhang, B., 2022. Effects of wet-media milling on

multi-scale structures and in vitro digestion of tapioca starch and the structure-digestion relationship. Carbohydr. Polym. 284, 119176. https://doi.org/10.1016/j.carbpol.2022.119176
Li, Y., He, Z., Tu, Y., Chen, L., Li, X., 2024. Understanding synchronous regulating effects of starch-protein interactions on starch digestion and retrogradation under thermal shear processing. Carbohydr. Polym. 329, 121767. https://doi.org/10.1016/j.carbpol.2023.121767
Li, Z., Di, H., Cheng, W., Zhang, Y., Ren, G., Ma, J., Yang, J., Huang, Z., Tang, Y., Zheng, Y., Li, H., Zhang, F., Sun, B., 2023. Variation in health-promoting compounds and antioxidant activities in mustard (Brassica juncea) sprouts. Sci. Hortic. 309, 111673. https://doi.org/10.1016/j.scienta.2022.111673
Lin, D., Zhao, J., Wang, Z., Qin, W., Wu, Z., 2023. Effects of glutathione on structural and digestibility properties of high-hydrostatic-pressure-gelatinized maize starch with different amylose/amylopectin ratios. LWT 115436. https://doi.org/10.1016/j.lwt.2023.115436
Lindeboom, N., Chang, P.R., Tyler, R.T., 2004. Analytical, Biochemical and Physicochemical Aspects of Starch Granule Size, with Emphasis on Small Granule Starches: A Review. Starch - Stärke 56, 89–99. https://doi.org/10.1002/star.200300218
Liu, L., Pan, Y., Zhang, X., Zhang, Y., Li, X., 2021. Effect of Particle Size and Interface Composition on the Lipid Digestion of Droplets Covered with Membrane Phospholipids. J. Agric. Food Chem. 69, 159–169. https://doi.org/10.1021/acs.jafc.0c04945
Liu, Q., Wang, Y., Yang, Y., Yu, X., Xu, L., Jiao, A., Jin, Z., 2023. Structure, physicochemical properties and in vitro digestibility of extruded starch-lauric acid complexes with different amylose contents. Food Hydrocoll. 136, 108239. https://doi.org/10.1016/j.foodhyd.2022.108239
Lu, Z.-H., Donner, E., Yada, R.Y., Liu, Q., 2016. Physicochemical properties and in vitro starch digestibility of potato starch/protein blends. Carbohydr. Polym. 154, 214–222. https://doi.org/10.1016/j.carbpol.2016.08.055
Luangsakul, N., Ritudomphol, O., 2018a. Effect of oil addition on in vitro starch digestibility and physicochemical properties of instant rice. Int. J. Agric. Technol. 14, 1399–1412.
Luangsakul, N., Ritudomphol, O., 2018b. Effect of oil addition on in vitro starch digestibility and physicochemical properties of instant rice. Int. J. Agric. Technol. 14, 1399–1412.
Mancini, A., Imperlini, E., Nigro, E., Montagnese, C., Daniele, A., Orrù, S., Buono, P., 2015. Biological and Nutritional Properties of Palm Oil and Palmitic Acid: Effects on Health. Molecules 20, 17339–17361. https://doi.org/10.3390/molecules200917339
McKenzie, K.M., Lee, C.M., Mijatovic, J., Haghighi, M.M., Skilton, M.R., 2021. Medium-Chain Triglyceride Oil and Blood Lipids: A Systematic Review and Meta-Analysis of Randomized Trials. J. Nutr. 151, 2949–2956. https://doi.org/10.1093/jn/nxab220
Ngadi, M., Li, Y., Oluka, S., 2007. Quality changes in chicken nuggets fried in oils with different degrees of hydrogenatation. LWT - Food Sci. Technol. 40, 1784–1791.

https://doi.org/10.1016/j.lwt.2007.01.004
Okumus, B.N., Tacer-Caba, Z., Kahraman, K., Nilufer-Erdil, D., 2018. Resistant starch type V formation in brown lentil (Lens culinaris Medikus) starch with different lipids/fatty acids. Food Chem. 240, 550–558. https://doi.org/10.1016/j.foodchem.2017.07.157
Paesani, C., Gómez, M., 2021. Effects of the pre-frying process on the cooking quality of rice. LWT 140, 110743. https://doi.org/10.1016/j.lwt.2020.110743
Pan, J., Li, M., Zhang, S., Jiang, Y., Lv, Y., Liu, J., Liu, Q., Zhu, Y., Zhang, H., 2019. Effect of epigallocatechin gallate on the gelatinisation and retrogradation of wheat starch. Food Chem. 294, 209–215. https://doi.org/10.1016/j.foodchem.2019.05.048
Pu, H., Chen, L., Li, L., Li, X., 2013. Multi-scale structural and digestion resistibility changes of high-amylose corn starch after hydrothermal-pressure treatment at different gelatinizing temperatures. Food Res. Int. 53, 456–463. https://doi.org/10.1016/j.foodres.2013.05.021
Quek, R., Henry, C.J., 2015. Influence of polyphenols from lingonberry, cranberry, and red grape on *in vitro* digestibility of rice. Int. J. Food Sci. Nutr. 66, 378–382. https://doi.org/10.3109/09637486.2015.1042849
Ramezanzadeh, F.M., Rao, R.M., Prinyawiwatkul, W., Marshall, W.E., Windhauser, M., 2000. Effects of Microwave Heat, Packaging, and Storage Temperature on Fatty Acid and Proximate Compositions in Rice Bran. J. Agric. Food Chem. 48, 464–467. https://doi.org/10.1021/jf9909609
Romano, A., D'Amelia, V., Gallo, V., Palomba, S., Carputo, D., Masi, P., 2018. Relationships between composition, microstructure and cooking performances of six potato varieties. Food Res. Int. 114, 10–19. https://doi.org/10.1016/j.foodres.2018.07.033
Santos, C.S.P., Molina-Garcia, L., Cunha, S.C., Casal, S., 2018. Fried potatoes: Impact of prolonged frying in monounsaturated oils. Food Chem. 243, 192–201. https://doi.org/10.1016/j.foodchem.2017.09.117
Sasaki, T., Kohyama, K., 2011. Effect of non-starch polysaccharides on the in vitro digestibility and rheological properties of rice starch gel. Food Chem. 127, 541–546. https://doi.org/10.1016/j.foodchem.2011.01.038
Shuai, X., Dai, T., Chen, M., Liang, R., Du, L., Chen, J., Liu, C., 2022. Comparative study on the extraction of macadamia (Macadamia integrifolia) oil using different processing methods. LWT 154, 112614. https://doi.org/10.1016/j.lwt.2021.112614
Singh, H., Sarkar, A., 2011. Behaviour of protein-stabilised emulsions under various physiological conditions. Adv. Colloid Interface Sci. 165, 47–57. https://doi.org/10.1016/j.cis.2011.02.001
Srichuwong, S., Sunarti, T.C., Mishima, T., Isono, N., Hisamatsu, M., 2005. Starches from different botanical sources I: Contribution of amylopectin fine structure to thermal properties and enzyme digestibility. Carbohydr. Polym. 60, 529–538. https://doi.org/10.1016/j.carbpol.2005.03.004
Su, Y., Zhang, M., Bhandari, B., Zhang, W., 2018. Enhancement of water removing and the quality of fried purple-fleshed sweet potato in the vacuum frying by combined power ultrasound and microwave technology. Ultrason. Sonochem. 44, 368–379.

https://doi.org/10.1016/j.ultsonch.2018.02.049
Sun, X., Sun, Z., Saleh, A.S.M., Zhao, K., Ge, X., Shen, H., Zhang, Q., Yuan, L., Yu, X., Li, W., 2021. Understanding the granule, growth ring, blocklets, crystalline and molecular structure of normal and waxy wheat A- and B- starch granules. Food Hydrocoll. 121, 107034. https://doi.org/10.1016/j.foodhyd.2021.107034
Suri, K., Singh, B., Kaur, A., Yadav, M.P., Singh, N., 2020. Influence of microwave roasting on chemical composition, oxidative stability and fatty acid composition of flaxseed (Linum usitatissimum L.) oil. Food Chem. 326, 126974. https://doi.org/10.1016/j.foodchem.2020.126974
Tamura, M., Hoshi, K., Saito, T., Sasahara, Y., 2022a. *In Vitro* Starch Digestion of Cooked Rice Grain Following the Addition of Various Vegetable Oils. Jpn. Agric. Res. Q. JARQ 56, 261–267. https://doi.org/10.6090/jarq.56.261
Tamura, M., Kumagai, C., Kaur, L., Ogawa, Y., Singh, J., 2021. Cooking of short, medium and long-grain rice in limited and excess water: Effects on microstructural characteristics and gastro-small intestinal starch digestion in vitro. LWT 146, 111379. https://doi.org/10.1016/j.lwt.2021.111379
Tamura, M., Kumagai, C., Ogawa, Y., 2022b. Influence of structural changes of brown rice by precise polishing on in vitro starch digestibility of cooked rice grain. Food Hydrocoll. Health 2, 100077. https://doi.org/10.1016/j.fhfh.2022.100077
Tamura M., Maehara N., Kumagai C., Saito H., Ogawa Y., 2019. Changes in Starch Digestibility and Tissue Structure of Cooked Rice Grain Under Different *In vitro* Simulated Gastric Digestive Conditions. Nippon Shokuhin Kagaku Kogaku Kaishi 66, 170–178. https://doi.org/10.3136/nskkk.66.170
Tamura, M., Saito, Y., Saito, T., Kobayashi, H., Mikami, A., Sasahara, Y., 2023. Multiple effects of oil addition and freezing-reheating treatment on the in vitro starch digestibility of rice grains. Food Hydrocoll. Health 4, 100150. https://doi.org/10.1016/j.fhfh.2023.100150
Tamura, M., Singh, J., Kaur, L., Ogawa, Y., 2019. Effect of post-cooking storage on texture and in vitro starch digestion of Japonica rice. J. Food Process Eng. 42, e12985. https://doi.org/10.1111/jfpe.12985
Tamura, M., Singh, J., Kaur, L., Ogawa, Y., 2016a. Impact of the degree of cooking on starch digestibility of rice – An in vitro study. Food Chem. 191, 98–104. https://doi.org/10.1016/j.foodchem.2015.03.127
Tamura, M., Singh, J., Kaur, L., Ogawa, Y., 2016b. Impact of structural characteristics on starch digestibility of cooked rice. Food Chem. 191, 91–97. https://doi.org/10.1016/j.foodchem.2015.04.019
Thanonkaew, A., Wongyai, S., McClements, D.J., Decker, E.A., 2012. Effect of stabilization of rice bran by domestic heating on mechanical extraction yield, quality, and antioxidant properties of cold-pressed rice bran oil (Oryza saltiva L.). LWT - Food Sci. Technol. 48, 231–236. https://doi.org/10.1016/j.lwt.2012.03.018
Thuengtung, S., Ketnawa, S., Ding, Y., Ogawa, Y., 2021. Effect of heat-moisture treatment to raw paddy rice (Oryza sativa L.) on cooked rice properties. J. Future Foods 1, 179–186. https://doi.org/10.1016/j.jfutfo.2022.01.007
Tochitani, Y., Fujimoto, M., 2001. Measurement of Specific Heat Capacity of

Vegetable Oils. Netsu Bussei 15, 230–236. https://doi.org/10.2963/jjtp.15.230
Torrijos, R., Righetti, L., Cirlini, M., Calani, L., Mañes, J., Meca, G., Dall'Asta, C., 2023. Phytochemical profiling of volatile and bioactive compounds in yellow mustard (Sinapis alba) and oriental mustard (Brassica juncea) seed flour and bran. LWT 173, 114221. https://doi.org/10.1016/j.lwt.2022.114221
Ulbricht, T.L.V., Southgate, D.A.T., 1991. Coronary heart disease: seven dietary factors. The Lancet 338, 985–992. https://doi.org/10.1016/0140-6736(91)91846-M
Wang, C., Su, G., Wang, X., Nie, S., 2019. Rapid Assessment of Deep Frying Oil Quality as Well as Water and Fat Contents in French Fries by Low-Field Nuclear Magnetic Resonance. J. Agric. Food Chem. 67, 2361–2368. https://doi.org/10.1021/acs.jafc.8b05639
Wang, F., Sun, Y., Li, S., Yan, J., Qin, W., Saleh, A.S.M., Zhang, Q., 2023. Plant phenolic extracts for the quality protection of frying oil during deep frying: Sources, effects, and mechanisms. Grain Oil Sci. Technol. 6, 148–161. https://doi.org/10.1016/j.gaost.2023.08.001
Wang, H., Wu, Y., Wang, N., Yang, L., Zhou, Y., 2019. Effect of water content of high-amylose corn starch and glutinous rice starch combined with lipids on formation of starch–lipid complexes during deep-fat frying. Food Chem. 278, 515–522. https://doi.org/10.1016/j.foodchem.2018.11.092
Wang, J., Zhao, S., Min, G., Qiao, D., Zhang, B., Niu, M., Jia, C., Xu, Y., Lin, Q., 2021. Starch-protein interplay varies the multi-scale structures of starch undergoing thermal processing. Int. J. Biol. Macromol. 175, 179–187. https://doi.org/10.1016/j.ijbiomac.2021.02.020
Wang, Shujun, Chao, C., Cai, J., Niu, B., Copeland, L., Wang, Shuo, 2020. Starch–lipid and starch–lipid–protein complexes: A comprehensive review. Compr. Rev. Food Sci. Food Saf. 19, 1056–1079. https://doi.org/10.1111/1541-4337.12550
Wang, Shujun, Wang, J., Yu, J., Wang, Shuo, 2016. Effect of fatty acids on functional properties of normal wheat and waxy wheat starches: A structural basis. Food Chem. 190, 285–292. https://doi.org/10.1016/j.foodchem.2015.05.086
Wickramasinghe Mudiyanselage, D.R., Wickramasinghe, I., 2023. Comparison of physicochemical characteristics of virgin coconut oils from traditional and hybrid coconut varieties. J. Agric. Food Res. 12, 100554. https://doi.org/10.1016/j.jafr.2023.100554
Wu, Y., Chen, Z., Li, X., Li, M., 2009. Effect of tea polyphenols on the retrogradation of rice starch. Food Res. Int. 42, 221–225. https://doi.org/10.1016/j.foodres.2008.11.001
Wu, Z.-W., Han, J.-Y., Zhao, X.-Y., Wei, Y.-Y., Cai, X.-S., Liu, H.-M., Ma, Y.-X., Wang, X.-D., 2024. Impact of high temperature on microstructural changes and oil absorption of tigernut (Cyperus esculentus L.) starch: Investigations in the starch-oil model system. Carbohydr. Polym. 328, 121711. https://doi.org/10.1016/j.carbpol.2023.121711
Xiang, C., Xu, Z., Liu, J., Li, T., Yang, Z., Ding, C., 2017. Quality, composition, and antioxidant activity of virgin olive oil from introduced varieties at Liangshan. LWT 78, 226–234. https://doi.org/10.1016/j.lwt.2016.12.029

Xiang, X., Wen, L., Wang, Z., Yang, G., Mao, J., An, X., Kan, J., 2023. A comprehensive study on physicochemical properties, bioactive compounds, and emulsified lipid digestion characteristics of Idesia polycarpa var. Vestita Diels fruits oil. Food Chem. 404, 134634. https://doi.org/10.1016/j.foodchem.2022.134634
Yang, C., Zhong, F., Douglas Goff, H., Li, Y., 2019. Study on starch-protein interactions and their effects on physicochemical and digestible properties of the blends. Food Chem. 280, 51–58. https://doi.org/10.1016/j.foodchem.2018.12.028
Yang, D., Wu, G., Li, P., Zhang, H., Qi, X., 2019. Comparative analysis of the oil absorption behavior and microstructural changes of fresh and pre-frozen potato strips during frying via MRl, SEM, and XRD. Food Res. Int. 122, 295–302. https://doi.org/10.1016/j.foodres.2019.04.024
Yang, D.S., Shewfelt, R.L., Lee, K.-S., Kays, S.J., 2008. Comparison of Odor-Active Compounds from Six Distinctly Different Rice Flavor Types. J. Agric. Food Chem. 56, 2780–2787. https://doi.org/10.1021/jf072685t
Yang, L., Sun, Y.-H., Liu, Y., Mao, Q., You, L.-X., Hou, J.-M., Ashraf, M.A., 2016. Effects of Leached Amylose and Amylopectin in Rice Cooking Liquidon Texture and Structure of Cooked Rice. Braz. Arch. Biol. Technol. 59. https://doi.org/10.1590/1678-4324-2016160504
Ye, S., Lu, H., 2022. Determination of Fatty Acids in Rice Oil by Gas Chromatography–Mass Spectrometry (GC–MS) with Geographic and Varietal Discrimination by Supervised Orthogonal Partial Least Squares Discriminant Analysis (OPLS-DA). Anal. Lett. 55, 675–687. https://doi.org/10.1080/00032719.2021.1960361
Ye, Z., Shang, Z., Li, M., Zhang, X., Ren, H., Hu, X., Yi, J., 2022. Effect of ripening and variety on the physiochemical quality and flavor of fermented Chinese chili pepper (Paojiao). Food Chem. 368, 130797. https://doi.org/10.1016/j.foodchem.2021.130797
Zabar, S., Lesmes, U., Katz, I., Shimoni, E., Bianco-Peled, H., 2009. Studying different dimensions of amylose–long chain fatty acid complexes: Molecular, nano and micro level characteristics. Food Hydrocoll. 23, 1918–1925. https://doi.org/10.1016/j.foodhyd.2009.02.004
Zhang, G., Venkatachalam, M., Hamaker, B.R., 2006. Structural Basis for the Slow Digestion Property of Native Cereal Starches. Biomacromolecules 7, 3259–3266. https://doi.org/10.1021/bm060343a
Zhang, Z., Tian, J., Fang, H., Zhang, H., Kong, X., Wu, D., Zheng, J., Liu, D., Ye, X., Chen, S., 2020. Physicochemical and Digestion Properties of Potato Starch Were Modified by Complexing with Grape Seed Proanthocyanidins. Molecules 25, 1123. https://doi.org/10.3390/molecules25051123
Zhao, X., Li, X., Guo, R., Wang, X., Zeng, L., Wen, X., Huang, Q., 2023. Different oil-modified cross-linked starches: In vitro digestibility and its relationship with their structural and rheological characteristics. Food Chem. 418, 135991. https://doi.org/10.1016/j.foodchem.2023.135991
Zhao, X., Wang, X., Li, X., Zeng, L., Huang, J., Huang, Q., Zhang, B., 2022a. Effect of oil modification on the multiscale structure and gelatinization properties of

crosslinked starch and their relationship with the texture and microstructure of surimi/starch composite gels. Food Chem. 391, 133236. https://doi.org/10.1016/j.foodchem.2022.133236
Zhao, X., Wang, X., Zeng, L., Huang, Q., Zhang, J., Wen, X., Xiong, S., Yin, T., Zhang, B., 2022b. Effects of oil-modified crosslinked/acetylated starches on silver carp surimi gel: Texture properties, water mobility, microstructure, and related mechanisms. Food Res. Int. 158, 111521. https://doi.org/10.1016/j.foodres.2022.111521
Zheng, Y., Tian, J., Kong, X., Wu, D., Chen, S., Liu, D., Ye, X., 2021. Proanthocyanidins from Chinese berry leaves modified the physicochemical properties and digestive characteristic of rice starch. Food Chem. 335, 127666. https://doi.org/10.1016/j.foodchem.2020.127666
Zheng, Y., Tian, J., Kong, X., Yang, W., Yin, X., Xu, E., Chen, S., Liu, D., Ye, X., 2020. Physicochemical and digestibility characterisation of maize starch–caffeic acid complexes. LWT 121, 108857. https://doi.org/10.1016/j.lwt.2019.108857

Acknowledgements

I would like to express my appreciation and gratitude to many individuals for their assistance and contributions towards the success of this thesis. First of all, I would like to express my thanks to the JST for providing a scholarship to me. My special gratitude is extended to my advisor, Prof. Dr. Yukiharu Ogawa for the continuous support of my Ph.D study and related research, for his patience, motivation, and immense knowledge. His guidance helped me in all the time of research and writing of this thesis. I could not have imagined having a better advisor and mentor for my Ph.D study. Besides my advisor, I would like to thank the rest of my thesis committee: Prof. Dr. Yukari Egashira, Prof. Dr. Shoko Hikosaka, and Prof. Dr. Yuya Fukano for their insightful comments and encouragement. My sincere thanks also go to Prof. Dr. Takeo Shiina and all laboratory members for their useful suggestions and comments though out the course of this research. Moreover, I would like to thank all staffs of the Graduate School of Horticulture, Chiba University for their kindness and support. I would like to thank my family for their love and encouragement.

List of Publication

Research articles:

1) **Wang, L.**, Hu, F., Bainto-Ancheta, L., Aumasa T., Wonglek S., Prempree p., Ogawa, Y. (2024). Structural characteristics and in vitro starch digestibility of oil-modified cooked rice with varied addition manipulations. *Food Research International, 186,* 114381.
2) Hu, F., **Wang, L.**, Bainto-Ancheta, L., Ogawa, Y. (2024). Effects of Matrix Structure on Protein Digestibility and Antioxidant Property of Different Soybean Curds During In Vitro Digestion. *Journal of Agricultural and Food Chemistry*,72, 7364‑7373.
3) **Wang, L.**, Cai, Y., Prempree, P., Hao, R., Jiang, D., Bainto-Ancheta, L., Ogawa, Y. (2024). Effect of adding various supplements on physicochemical properties and starch digestibility of cooked rice. *Scientific Report*, 14, 24606.

Conferences:

1) **Wang, L.**, Hu, F., Ogawa, Y. Investigation of structural and in vitro digestibility of rice starch with varied oil types and addition manipulation. Joint Conference on Environmental Engineering in Agriculture 2023, 4-8 September 2023. Tsukuba University, Tsukuba, Japan.

2) Hu, F., **Wang, L.**, Ogawa, Y. A comparison study on the structure and bioaccessibility of different types of tofu. Joint Conference on Environmental Engineering in Agriculture 2023, 4-8 September 2023. Tsukuba University, Tsukuba, Japan.